Proceedings of SPIE Conference on Signal and Data Processing
of Small Targets, San Diego, CA, USA, July-August 2001. (4473-63)

A Survey of Maneuvering Target Tracking—Part II: Ballistic Target Models*

X. Rong Li and **Vesselin P. Jilkov**
Department of Electrical Engineering
University of New Orleans
New Orleans, LA 70148, USA
504-280-7416 (phone), 504-280-3950 (fax), xli@uno.edu, vjilkov@uno.edu

Abstract

This paper is the second part in a series that provides a comprehensive survey of the problems and techniques of tracking maneuvering targets in the absence of the so-called measurement-origin uncertainty. It surveys motion models of ballistic targets used for target tracking. Models for all three phases (i.e., boost, coast, and reentry) of motion are covered.

Key Words: Target Tracking, Maneuvering Target, Dynamics Model, Ballistic Target, Survey

1 Introduction

A survey of dynamics models used in maneuvering target tracking has been reported in [1]. It, however, does not cover motion models used for tracking ballistic targets (BT), that is, ballistic missiles, decoys, debris, and satellites. The primary reason for this omission is that these models possess many distinctive features that differ vastly from those covered in [1]. To supplement [1], a survey of these models is presented in this paper. To our knowledge, such a survey is not available in the literature. Measurement models are surveyed in Part III [2].

The entire trajectory of a BT, from launch to impact, is commonly divided into three basic phases [3, 4]: *boost* [1], *ballistic* (also known as *coast*), and *reentry*. The boost phase of motion is the powered, endo-atmospheric flight, which lasts from launch to thrust cutoff or burnout. It is followed by the ballistic phase, which is an exo-atmospheric, free-flight motion, continuing until the Earth's atmosphere is reached again. The atmospheric *reentry* begins when the atmospheric drag becomes considerable and endures until impact.

Target dynamics during the different phases are substantially different. A succinct ouline of the main dynamic phases is given in [5]. The boost phase is characterized by a large (primarily axial) thrust acceleration, which in the case of rocket staging is subject to abrupt, jump-wise changes. The effects of the atmospheric drag and the Earth's gravity are also essential in this phase. After the boost (i.e., during the post-boost), drag is no longer present and the level of thrust becomes low or vanishes. During the exo-atmospheric ballistic phase the motion is governed essentially by the Earth's gravity only — the trajectory is more predictable, still, small re-targeting maneuvers are possible. The reentry phase features a rapid drag deceleration with possible lateral accelerations.

Overall, a ballistic target has a less uncertain motion than many other types of powered vehicles, such as maneuvering aircraft or agile missiles: Most BTs follow a flight path that is to a large extent predetermined by the performance characteristics, specific for a target type, hence the name *ballistic* targets. Only some more advanced missiles can undergo small maneuvers, usually for re-targeting. However, this does not mean that the motion of a foreign target can be determined accurately. In fact, as vividly expressed in [4], tracking a foreign BT is likely to be "plagued" with a variety of uncertainties, including those concerning trajectory loft or depression, thrust profile management, target weight, propellant specific impulse, sensor bias, and atmospheric parameters. Many of these uncertainties stem from the uncertainty in the target/missile type, the principal uncertainty in modeling the motion of a foreign BT for the tracking purpose.

Compared with [1], this survey is slightly more tutorial in nature for the benefit of the readers less familiar with the ballistics or aerodynamics. The same disclaimers as made in the Introduction section of [1] apply to this survey, including those on the restriction to point targets for temporal behaviors and the interrelationship between dynamics models and tracking algorithms. The reader should keep in mind that while there have been many extensive studies of BT tracking, not many

*Research supported by ONR Grant N00014-00-1-0677 and NSF Grant ECS-9734285.

[1] And possibly a post-boost phase, which involves small maneuvers.

results have been published in the open literature. In other words, much of the BT information, particularly target-type specific information, such as motion profiles (or templates), is classified and not open to the general public. As a result, this survey covers only those dynamics models used for BT tracking in the open literature available to us. While some models covered are applicable to satellite tracking, the emphasis of the survey is on missile tracking.

The rest of the paper is organized as follows. Sec. 2 provides background knowledge in ballistics and aerodynamics that is necessary to understand the BT motion models presented later. Motion models for the simplest phase, the ballistic flight, are covered in Sec. 3. This is followed in Sec. 4 by a survey of the models for reentry vehicles. Sec. 5 then describes models for the boost phase, the most sophisticated phase.

2 Preliminaries

In this section, we provide necessary, rudimentary background information in aerodynamics and ballistics to help the reader understand the BT motion models presented in the subsequent sections. We hope this will make the text more systematic and self-contained.

2.1 Coordinate Systems

The coordinate systems (CS) commonly used in BT tracking are illustrated in Fig. 1. Much more detailed information on coordinate systems can be found in e.g. [4, 6, 7, 8, 9, 10].

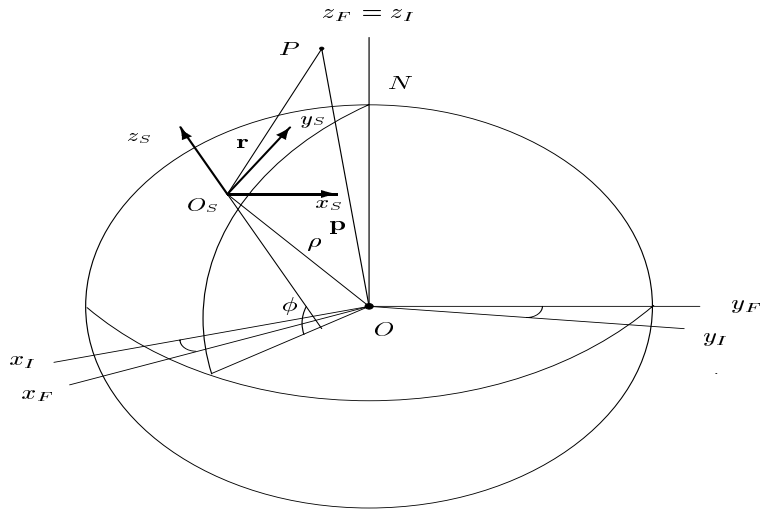

Fig. 1: Coordinate Systems

The *Earth-centered inertial* (ECI) CS $Ox_Iy_Iz_I$ is fixed in an inertial space (i.e., fixed relative to the "fixed stars"). It is a right-handed system with the origin O at the Earth center, axis Ox_I pointing in the vernal equinox direction, axis Oz_I pointing in the direction of the North pole N. Its fundamental plane Ox_Iy_I coincides with the Earth's equatorial plane.

The *Earth-centered (Earth) fixed* (ECF, ECEF, or ECR) CS $Ox_Fy_Fz_F$ also has its origin at the Earth center O, its axis $z_F \equiv z_I$, and fundamental plane Ox_Fy_F coincident with the Earth's equatorial plane. Its axes Ox_F and Oy_F, however, *rotate* with the Earth around the Earth's spin axis $Oz_F \equiv Oz_I$ as Ox_F points to the prime meridian.

The *East-North-Up* (ENU) CS $O_Sx_Sy_Sz_S$ has its origin O_S at some point on the Earth surface or above it (usually at the location of a sensor). Its Up-axis $O_S\ z_S$ is normal to the Earth's reference ellipsoid,[2] usually defined by the geodetic latitude ϕ. The axes O_Sx_S and O_Sy_S are tangential to the Earth reference ellipsoid with y_S pointing North and x_S East.

Another CS (not depicted in Fig. 1), commonly used in BT tracking, is the *radar face* (RF) CS [3] [11, 6]. It can be defined from the local radar ENU-CS by two angles of rotation [6]. For a phased array radar, the x and y axes of the RF-CS lie on the radar face, with x axis along the intersection of the radar face with the local horizontal plane, and z is along its normal

[2] Note that the local vertical direction differs from the radial axis $\overrightarrow{OO_S}$. They coincide if a spherical Earth model is used.

[3] Note that it differs from the so-called radar reference CS, which is actually just an ENU-CS at radar site [11].

(boresight) direction. Such a radar measures the range $r = \sqrt{x^2 + y^2 + z^2}$ and the direction cosines $u = x/r$ and $v = y/r$. This nonorthogonal coordinate system (r, u, v) is often referred to as the *RUV-CS*.

In Fig. 1**,** points P and O_S (i.e., vectors $\mathbf{p} \triangleq \overrightarrow{OP}$ and $\boldsymbol{\rho} \triangleq \overrightarrow{OO_S}$) denote target and sensor positions in the ECI-CS or ECF-CS, respectively. Vector $\mathbf{r} \triangleq \overrightarrow{O_S P}$ defines the target position with respect to the sensor in the ENU-CS.

Note that the velocity in the ECF-CS can be expressed in the ECI-CS as follows

$$\dot{x}_F = \dot{x}_I - \omega_e y_I, \quad \dot{y}_F = \dot{y}_I + \omega_e x_I, \quad \dot{z}_F = \dot{z}_I \tag{1}$$

where ω_e is the Earth rotation rate.

The choice of a CS is a complex issue, depending on numerous factors and related with many elements of a tracking system [9, 10]. For more information, the reader is referred to [2].

2.2 Total Acceleration

For the tracking purpose, only the most substantial forces that may act on a BT are considered: *thrust*, aerodynamic forces (most notably, atmospheric *drag* and possibly *lift*), the Earth's *gravity*, and, depending on the CS used, possibly the Coriolis and centrifugal forces. Not all these forces are present at a level that affects significantly the motion of a BT in the different regimes of the trajectory. Specifically, for most tracking applications the significant forces in difference phases are

- **Boost:** Thrust, drag, and gravity.
- **Coast:** Gravity only.
- **Reentry:** Gravity, drag, and lift.

The total acceleration of a BT, in the ECI-CS in a fairly general setting, can be decomposed as

$$\mathbf{a} = \mathbf{a}_T + \underbrace{\mathbf{a}_D + \mathbf{a}_L}_{\mathbf{a}_A} + \mathbf{a}_G \tag{2}$$

where $\mathbf{a}_T$, $\mathbf{a}_A$ $(\mathbf{a}_D, \mathbf{a}_L)$, and $\mathbf{a}_G$ denote the acceleration components induced by thrust, aerodynamic forces (drag and lift), and gravity, respectively. Note that the acceleration here is expressed in the ECI-CS (i.e., $\mathbf{a} \triangleq d^2\mathbf{p}/dt^2$) in the *absolute* sense. If the target motion is considered within a frame fixed to the Earth (e.g., the ENU-CS), then its *relative* total acceleration $\mathbf{a}_r$ (defined as $\mathbf{a}_r \triangleq \frac{d}{dt}\mathbf{v}_r$ for $\mathbf{v}_r \triangleq \frac{d}{dt}\mathbf{r}$) should be corrected with the accelerations induced by the Earth's rotation [3, 4]:

$$\mathbf{a}_r = \mathbf{a} - \underbrace{2\boldsymbol{\omega}_e \times \mathbf{v}_r}_{\textit{Coriolis}} - \underbrace{\boldsymbol{\omega}_e \times (\boldsymbol{\omega}_e \times (\mathbf{r} + \boldsymbol{\rho}))}_{\textit{Centrifugal}} \tag{3}$$

where $\boldsymbol{\omega}_e$ is the Earth's angular velocity vector. The terms $2\boldsymbol{\omega}_e \times \mathbf{v}$ and $\boldsymbol{\omega}_e \times (\boldsymbol{\omega}_e \times (\mathbf{r} + \boldsymbol{\rho}))$ represent the accelerations due to the Coriolis[4] and centrifugal forces, respectively.

Clearly, the entire end-to-end motion of a BT can be modeled by a "wide-band" dynamic model (e.g., nearly constant velocity, acceleration, jerk, or Singer model [1]) capable of covering the whole range of possible trajectories. Most models developed for the boost phase, the most sophisticated of all three phases, can serve this purpose. This is, however, rather crude and not in common use. What is more natural and rational, as well as common practice, is to develop different models specific for each trajectory portion that more fully exploit the inherent characteristics of the portion.

We survey next dynamics models for the distinct regimes of a BT proposed/used in the available literature. The motion phases are ordered with respect to their sophistication levels, rather than to their chronology in the trajectory.

[4]The Coriolis force is an equivalent force induced by the rotation of the Earth that causes the Coriolis effect — the apparent deflection of a body in motion with respect to the Earth, as seen by an observer on the Earth.

3 Ballistic (Coast) Flight

After the thrust cut-off or burnout and leaving the atmosphere a BT enters the free-flight portion of its trajectory — no thrust is applied and no drag is experienced. The motion may be considered governed by the gravity alone — other factors (e.g., perturbations) are neglected. By (2) the total acceleration is $\mathbf{a} = \mathbf{a}_G$ and thus obtaining a coast model of the BT amounts to selection of an appropriate gravity model.

3.1 Gravity Models

Flat Earth Model. The simplest possible model of gravity assumes a flat, nonrotating Earth. In this model, the gravity acting on the target in the ENU-CS is $\mathbf{a}_G = \mathbf{g}_0 = [0, 0, -g]'$, where g is the constant gravitational acceleration of the Earth.

The boost and reentry portions of a BT trajectory are relatively short in range compared to the Earth radius and take place in a close vicinity of the Earth. Thus a model of flat, non-rotating Earth may be adequate, particularly in view of the presence of other more dominating uncertainties. On the contrary, the coast flight comprises much greater ranges usually and thus accounting for the Earth sphericity (and even ellipticity) and rotation is essential.

Spherical Earth Model. Assume that the Earth and the BTs can be represented as point masses at their geocenters[5] and that the gravitational forces of the moon (and other stars) can be neglected. Since the target has a negligible mass relative to the Earth's mass, the gravitational acceleration $\mathbf{a}_G$ is the solution of a so-called restricted two-body problem, obtained by the Newton's inverse-square gravity law [4] as

$$\mathbf{a}_G(\mathbf{p}) = -\frac{\mu}{p^2}\mathbf{u}_p = -\frac{\mu}{p^3}\mathbf{p} \tag{4}$$

where $\mathbf{p}$ is the vector from the Earth center to the target, $p \triangleq \|\mathbf{p}\|$ is its length, $\mathbf{u}_p \triangleq \mathbf{p}/p$ is the unit vector in the direction of $\mathbf{p}$, and μ is the Earth's gravitational constant[6].

This *inverse-square gravitational acceleration model* (4) is classical and has been commonly used in a variety of BT tracking applications [12, 13, 14, 15, 16, 17, 18, 19, 9]. It is attractive for its simplicity. It has been proven satisfactory for tracking of BTs over a short range and/or period, for example, as a model of the gravitational acceleration as an integral part of the total acceleration within a boost (boost-to-coast) motion model [15, 16, 19, 9] or for track initiation purposes [17]. However, its underlying assumptions are rather idealistic, especially the one that the Earth can be treated as a point mass. This may make it inadequate for other BT tracking applications, in particular, precision tracking of coast targets over a long time period or at a low data rate, such as the ballistic flight portion of a long-range missile or a satellite. Clearly, these simplifying assumptions becomes less accurate when the targets being tracked travel over a larger geographical region and a longer time period. Also, during the exo-atmospheric ballistic flight, gravity is either the only practical or at least the dominating acceleration acting on the targets and thus needs to be modeled more accurately. That is why the employment of more precise gravity models have been proposed.

Ellipsoidal Earth Model. More accurate expressions for the gravitational acceleration can be obtained by replacing the above spherical Earth model with an ellipsoidal (or more precisely, spheroidal) Earth model. Such a more precise approximation — accounting for the Earth oblateness by including the second-order gravitational harmonic term J_2 of the Earth's gravitational field model — is [4, 11]

$$\mathbf{a}_G(\mathbf{p}) = -\frac{\mu}{p^2}\left\{\mathbf{u}_p + \frac{3}{2}J_2\left(\frac{r_e}{p}\right)^2\left[\left(1 - 5\left(\mathbf{u}'_p \cdot \mathbf{u}_z\right)^2\right)\mathbf{u}_p + 2\left(\mathbf{u}'_p \cdot \mathbf{u}_z\right)\mathbf{u}_z\right]\right\} \tag{5}$$

where r_e is the Earth's equatorial radius, J_2 is a correction constant, and $\mathbf{u}_z$ is the unit vector along $\overrightarrow{Oz_I}$ (see Fig. 1). J_2, the best known Jeffery constant, represents the difference between the polar and equatorial moment of inertia. It quantifies the oblateness of the Earth because it is approximately equal to one third of the ellipticity of the Earth, hence also known as the oblateness term. This model is usually considered sufficiently accurate for most BT tracking applications [11], at a cost of considerable nonlinearity.

[5] This holds if the Earth and the targets are spherically symmetric with an even distribution of their masses.

[6] For the values of well-known constants used in this survey, the reader is referred to [4].

3.2 Motion Models in ECI Coordinates

In the ECI-CS, the target position and velocity vectors are $\mathbf{p} = (x, y, z)'$ and $\mathbf{v} \triangleq \dot{\mathbf{p}} = (\dot{x}, \dot{y}, \dot{z})'$ respectively. Clearly, a state-space model of a coast target with the state vector $\mathbf{x} = (\mathbf{p}', \mathbf{v}')'$ *in the ECI-CS* is

$$\dot{\mathbf{x}} \triangleq \begin{bmatrix} \dot{\mathbf{p}} \\ \dot{\mathbf{v}} \end{bmatrix} = \mathbf{f}\left(\begin{bmatrix} \mathbf{p} \\ \mathbf{v} \end{bmatrix}\right) \triangleq \begin{bmatrix} \mathbf{v} \\ \mathbf{a}_G(\mathbf{p}) \end{bmatrix} \tag{6}$$

where $\mathbf{a}_G(\mathbf{p})$ is the gravitational acceleration given by, e.g., (4) or (5).

3.2.1 Inverse-Square Model

In this case, the *acceleration part* of the state-space model (6) is clearly described by the inverse-square model (4) in the ECI-CS as:

$$\begin{bmatrix} \ddot{x} \\ \ddot{y} \\ \ddot{z} \end{bmatrix} = -\frac{\mu}{p^3}\begin{bmatrix} x \\ y \\ z \end{bmatrix} \quad \text{with} \quad p \triangleq \|\mathbf{p}\| = \sqrt{x^2 + y^2 + z^2} \tag{7}$$

A trajectory described by (6) with (7) is confined to a plane in the ECI-CS, called an orbital plane, and is a part of a conic orbit, governed by the Keplerian motion equation [4]. For the BTs considered in this survey, this orbit is elliptical.

A dynamics model is mainly used in target tracking for propagating the target state (i.e., state prediction), known as the Kepler problem in astrodynamics, and covariance prediction. While the model of (6) with (7) is highly nonlinear, with it the state propagation can be done in an efficient manner, as outlined below.

Given $\mathbf{x}(t_0) = (\mathbf{p}_0', \mathbf{v}_0')'$ at time t_0 the (predicted) target state $\mathbf{x}(t) = (\mathbf{p}', \mathbf{v}')'$ at time $t = t_0 + T$ (with $T > 0$) is given by [4]

$$\mathbf{p} = \left(1 - \frac{\lambda^2}{p_0}C\right)\mathbf{p}_0 + \left(T - \frac{\lambda^3}{\sqrt{\mu}}S\right)\mathbf{v}_0 \tag{8}$$

$$\mathbf{v} = \frac{\sqrt{\mu}\lambda(\zeta S - 1)}{p_0 p}\mathbf{p}_0 + \left(1 - \frac{\lambda^2 C}{p_0}\right)\mathbf{v}_0 \tag{9}$$

where C, S, and ζ are known functions of λ. The variable λ is defined through its time derivative by $\dot{\lambda} \triangleq \frac{\sqrt{\mu}}{p}$ and can be computed accurately and efficiently via the Newton iteration scheme for solving a so-called time-of-flight equation, as given below for the case of an elliptical orbit (i.e., $a \triangleq \frac{2}{p_0} - \frac{v_0^2}{\mu} > 0$) [4]:

1. Initialize

$$\alpha := \frac{1 - ap_0}{\sqrt{\mu}}, \quad \beta := \frac{\mathbf{p}_0' \cdot \mathbf{v}_0}{\mu}, \quad \lambda := \frac{aT}{\sqrt{\mu}}, \quad \gamma := \frac{p_0}{\sqrt{\mu}}$$

2. Repeat

$$\begin{aligned} \zeta &:= a\lambda^2 \\ C &:= \frac{1 - \cos\sqrt{\zeta}}{\zeta} \\ S &:= \frac{\sqrt{\zeta} - \sin\sqrt{\zeta}}{\zeta\sqrt{\zeta}} \\ \tau &:= \alpha\lambda^3 S + \beta\lambda^2 C + \gamma\lambda \\ \frac{d\tau}{d\lambda} &:= \alpha\lambda^2 C + \beta\lambda(1 - \zeta S) + \gamma \\ \lambda &:= \left[\frac{d\tau}{d\lambda}\right]^{-1}(T - \tau) \end{aligned}$$

Until $|T - \tau| < \epsilon$

A useful program-like pseudocode[7] of the above algorithm for all conic (i.e., elliptical, parabolic, and hyperbolic) trajectories can be found in [17], along with the computation of the Jacobian $F(t, t_0) = \partial\mathbf{x}(t)/\partial\mathbf{x}(t_0)$ necessary for the extended

[7] With a few small typographical errors.

Kalman filtering (EKF) [13, 20]. Explicit evaluation of the Jacobian by direct differentiation of (7) can be found in [14]. For a comprehensive treatment of the underlying theoretical background and solutions to the Kepler prediction problem, the reader is referred to [4].

3.2.2 Model with J_2 Correction

A refined model for the gravitational acceleration is based on the ellipsoidal Earth model (5). Note that $\mathbf{u}_p \triangleq [x,\ y,\ z]'/p$ and $\mathbf{u}_z = [0,\ 0,\ 1]'$ in the ECI-CS. Similar to (7), the acceleration part of the state-space model (6) has the following form [4, 16]:

$$\begin{bmatrix} \ddot{x} \\ \ddot{y} \\ \ddot{z} \end{bmatrix} = -\frac{\mu}{p^3} \begin{bmatrix} \left(1 + \frac{c_e}{p^2}\left(1 - 5\left(\frac{z}{p}\right)^2\right)\right) x \\ \left(1 + \frac{c_e}{p^2}\left(1 - 5\left(\frac{z}{p}\right)^2\right)\right) y \\ \left(1 + \frac{c_e}{p^2}\left(3 - 5\left(\frac{z}{p}\right)^2\right)\right) z \end{bmatrix} \quad \text{with} \quad c_e \triangleq \frac{3}{2} J_2 r_e^2 \tag{10}$$

This model is highly accurate. It was chosen as the coast model for a 6-state EKF-based ballistic filter in the ECI-CS implemented in a multiple-model tracking system developed in [16, 5]. However, as pointed out in [16], a model mismatch caused by moderate trajectory perturbations (due to, e.g., maneuvers from countermeasure thrust) will lead to track divergence. This effect can be alleviated by introducing small fictitious zero-mean process noise. This technique was used in [16] to adapt the model for the post-boost phase of the trajectory, where small maneuvers are involved.

In the early work on BT (e.g., satellite) tracking and in particular orbit determination, the target dynamics were usually considered to be deterministic (i.e., without process noise). This often had led to divergence problems with the EKF [13]. Introducing a fictitious process noise input is an effective means to account for such factors as model errors, neglected perturbations, nonlinearities, and computer roundoff errors. With an additional zero-mean process noise input, while state prediction is unaffected, its associated error covariance is amplified by the process noise covariance Q, thus reducing the possibility for the EKF to diverge. The price paid is a possible accuracy degradation of the filter when the deterministic model is indeed adequate. This is closely related to the problem of noise identification and adaptive filtering. See [13] and the brief surveys included in [21, 22]. The latest work along this line for tracking an orbital target can be found in [23], where Q is tuned adaptively using the most recent state estimate and covariance, as well as gravity-gradient model with the inverse-square law. Although a number of choices of Q have been proposed in the literature, Q remains a design parameter in practice, adjusted/tuned mostly based on engineering experience and intuition [11, 24].

3.3 Motion Models in ENU Coordinates

It is often preferable or necessary to formulate the BT motion in the *natural* sensor ENU coordinate system (Fig. 1). For this reason, let $\mathbf{r} \triangleq [x,\ y,\ z]'$, $\mathbf{v} \triangleq \dot{\mathbf{r}} = [\dot{x},\ \dot{y},\ \dot{z}]'$, and $\mathbf{a} \triangleq \dot{\mathbf{v}} = \ddot{\mathbf{r}} = [\ddot{x},\ \ddot{y},\ \ddot{z}]'$ denote the target position, velocity, and acceleration in the ENU CS respectively. In this case the total acceleration $\mathbf{a}$ involves the *Coriolis* and *centrifugal* terms as well as the gravitational acceleration $\mathbf{a}_G(\mathbf{p})$:

$$\mathbf{a}(\mathbf{p}, \mathbf{v}) = \mathbf{a}_G(\mathbf{p}) - \mathbf{a}_C^{(1)}(\mathbf{v}) - \mathbf{a}_C^{(2)}(\mathbf{p}) \tag{11}$$

with

$$\mathbf{a}_C^{(1)}(\mathbf{v}) \triangleq \underbrace{2\boldsymbol{\omega}_e \times \mathbf{v}}_{\textit{Coriolis}} \quad \text{and} \quad \mathbf{a}_C^{(2)}(\mathbf{p}) \triangleq \underbrace{\boldsymbol{\omega}_e \times (\boldsymbol{\omega}_e \times \mathbf{p})}_{\textit{Centrifugal}} \tag{12}$$

where the vector $\mathbf{p} = \mathbf{r} + \boldsymbol{\rho}$ and the Earth's angular velocity vector $\boldsymbol{\omega}_e = [\omega_x,\ \omega_y,\ \omega_z]'$ are expressed *in the ENU-CS* (see, e.g., [4]).

During the powered-flight and reentry portions of a BT, where the target is in a close vicinity of the Earth and over a short period, the effect of the Coriolis and centrifugal forces may be neglected compared with other factors. For the ballistic portion, however, this effect on the BT motion relative to a non-inertial frame (e.g., the ENU-CS) is usually significant and should be accounted for, in particular, in the case of long-range BTs (relative to the Earth's radius).

The target state-space model in the ENU-CS is clearly given by

$$\dot{\mathbf{x}} \triangleq \begin{bmatrix} \dot{\mathbf{r}} \\ \dot{\mathbf{v}} \end{bmatrix} = \mathbf{f}\left(\begin{bmatrix} \mathbf{r} \\ \mathbf{v} \end{bmatrix}\right) \triangleq \begin{bmatrix} \mathbf{v} \\ \mathbf{a}(\mathbf{r} + \boldsymbol{\rho}, \mathbf{v}) \end{bmatrix} \tag{13}$$

where $\mathbf{a}$ is the total acceleration, as a function of the position $\mathbf{r}$ and velocity $\mathbf{v}$, specified by (11) and (12).

3.3.1 Inverse-Square Model

With this spherical Earth model, as shown in Fig. 1, the vector $\overrightarrow{OP}$ from the Earth center to the target in the ENU-CS is $\mathbf{p} = \mathbf{r} + \boldsymbol{\rho} = (x,\, y,\, z)' + (0,\, 0,\, \rho)' = (x,\, y,\, z + \rho)'$, where $\rho = r_e + z_S$ is the *known* distance between the sensor and the Earth center, $\boldsymbol{\omega}_e = \omega_e\,(0, \cos\phi, \sin\phi)'$, ω_e is the Earth rotation rate, ϕ and z_S are the known sensor latitude and altitude, respectively, and r_e is the Earth center. Then it can be easily obtained from (12) that

$$\mathbf{a}_C^{(1)}\,(\mathbf{v}) \;=\; 2\omega_e \begin{bmatrix} -\dot{y}\sin\phi + \dot{z}\cos\phi \\ \dot{x}\sin\phi \\ -\dot{x}\cos\phi \end{bmatrix} = 2\omega_e \Phi \mathbf{v}, \tag{14}$$

$$\mathbf{a}_C^{(2)}\,(\mathbf{p}) \;=\; \omega_e^2 \begin{bmatrix} -x \\ [-y\sin\phi + (z+\rho)\cos\phi]\sin\phi \\ [y\sin\phi - (z+\rho)\cos\phi]\cos\phi \end{bmatrix} = \omega_e^2 \Phi^2 \mathbf{p} \tag{15}$$

where

$$\Phi \triangleq \begin{bmatrix} 0 & -\sin\phi & \cos\phi \\ \sin\phi & 0 & 0 \\ -\cos\phi & 0 & 0 \end{bmatrix}, \quad \Phi^2 = \begin{bmatrix} -1 & 0 & 0 \\ 0 & -\sin^2\phi & \sin\phi\cos\phi \\ 0 & \sin\phi\cos\phi & -\cos^2\phi \end{bmatrix} \tag{16}$$

Thus the motion equation can be given in the following compact form

$$\begin{bmatrix} \ddot{x} \\ \ddot{y} \\ \ddot{z} \end{bmatrix} = \mathbf{g}_1(\mathbf{x}) \triangleq -\left(\frac{\mu}{p^3} I + \omega_e^2 \Phi^2\right) \begin{bmatrix} x \\ y \\ z+\rho \end{bmatrix} - 2\omega_e \Phi \begin{bmatrix} \dot{x} \\ \dot{y} \\ \dot{z} \end{bmatrix} \tag{17}$$

with $p \triangleq \sqrt{x^2 + y^2 + (z+\rho)^2}$.

As for the models considered before, the standard EKF technique is directly applicable to this model in the ENU-CS. The linearization needed for error covariance propagation is sufficiently accurate for relatively short propagation time periods. For cases with high sampling rates, however, a simple yet accurate piecewise-constant acceleration model [18] could be used, discussed later.

3.3.2 Model with J_2 Correction

With an ellipsoidal Earth model in the sensor ENU-CS (see, e.g., [10]), the vector from the Earth center to the target is $\mathbf{p} = \mathbf{r} + \boldsymbol{\rho} = \left(x + \rho_x,\, y + \rho_y,\, z + \rho_z\right)'$, where $\boldsymbol{\rho} = \left(\rho_x, \rho_y, \rho_z\right)' \neq (0, 0, \rho)'$. It is then straightforward to obtain the state-space form of the acceleration model in the sensor ENU-CS from (11) with (5) and (12) as

$$\begin{bmatrix} \ddot{x} \\ \ddot{y} \\ \ddot{z} \end{bmatrix} = \mathbf{g}_2(\mathbf{x}) \triangleq -\frac{\mu}{p^3} \begin{bmatrix} \left(1 + \frac{c_e}{p^2}\left(1 - 5\left(\frac{z+\rho_z}{p}\right)^2\right)\right)(x+\rho_x) \\ \left(1 + \frac{c_e}{p^2}\left(1 - 5\left(\frac{z+\rho_z}{p}\right)^2\right)\right)(y+\rho_y) \\ \left(1 + \frac{c_e}{p^2}\left(3 - 5\left(\frac{z+\rho_z}{p}\right)^2\right)\right)(z+\rho_z) \end{bmatrix} - 2\Omega \begin{bmatrix} \dot{x} \\ \dot{y} \\ \dot{z} \end{bmatrix} - \Omega^2 \begin{bmatrix} x+\rho_x \\ y+\rho_y \\ z+\rho_z \end{bmatrix} \tag{18}$$

with

$$p \triangleq \sqrt{\left(x+\rho_x\right)^2 + \left(y+\rho_y\right)^2 + \left(z+\rho_z\right)^2} \quad \text{and} \quad \Omega \triangleq \begin{bmatrix} 0 & -\omega_z & \omega_y \\ \omega_z & 0 & -\omega_x \\ -\omega_y & \omega_x & 0 \end{bmatrix} \tag{19}$$

The Jacobian of the model needed for the state prediction error covariance can be computed as [11]

$$F = \frac{d\mathbf{f}}{d\mathbf{x}} = \begin{bmatrix} 0_{3\times 3} & I_{3\times 3} \\ -\frac{\mu}{p^3}\left(I_{3\times 3} - \frac{3}{p^2}\mathbf{p}\mathbf{p}'\right) - \Omega^2 & -2\Omega \end{bmatrix} \tag{20}$$

By including the J_2 correction term, this model clearly gives a more accurate approximation of the gravitational acceleration than the simper spherical Earth based models. A detailed discussion of its further conversion to the radar face CS and the corresponding RUV-CS and of its application in the EKF can be found in [11]. A similar model with inverse-square gravity, an ellipsoidal Earth, and Coriolis and centrifugal acceleration terms in the radar face CS, along with the respective EKF with RUV measurements is discussed in [6].

3.3.3 Piecewise-Constant Acceleration Model

The idea of this approach, proposed in [18], is simple and natural. At each propagation time step $t_k \rightarrow t_{k+1}$, first sample (i.e., compute) the continuous-time total acceleration process at the estimated point $\hat{\mathbf{x}}(t_k|t_k) = [\hat{x}, \hat{\dot{x}}, \hat{y}, \hat{\dot{y}}, \hat{z}, \hat{\dot{z}}]'$, that is, $\hat{\mathbf{a}}(t_k|t_k) = \mathbf{a}[\hat{\mathbf{x}}(t_k|t_k)]$. For example, if (17) is used to model the total acceleration, we have

$$\hat{\mathbf{a}}(t_k|t_k) = \begin{bmatrix} \hat{\ddot{x}} \\ \hat{\ddot{y}} \\ \hat{\ddot{z}} \end{bmatrix}(t_k|t_k) = \mathbf{g}_1[\hat{\mathbf{x}}(t_k|t_k)] = -\left(\frac{\mu}{\hat{p}^3} I + \omega_e^2 \Phi^2\right) \begin{bmatrix} \hat{x} \\ \hat{y} \\ \hat{z} + \rho \end{bmatrix} - 2\omega_e \Phi \begin{bmatrix} \hat{\dot{x}} \\ \hat{\dot{y}} \\ \hat{\dot{z}} \end{bmatrix} \tag{21}$$

with $\hat{p} = \sqrt{\hat{x}^2 + \hat{y}^2 + (\hat{z} + \rho)^2}$. Then, assume that the target motion is uncoupled along x, y, and z directions with a constant acceleration $\mathbf{a}(t) = [\ddot{x}(t), \ddot{y}(t), \ddot{z}(t)]' = \hat{\mathbf{a}}(t_k|t_k)$ over the time period $[t_k, t_{k+1})$. This leads to the following discrete-time dynamics model, for example, along the x direction

$$\begin{bmatrix} x \\ \dot{x} \end{bmatrix}(t_{k+1}) = \begin{bmatrix} 1 & t_{k+1} - t_k \\ 0 & 1 \end{bmatrix} \begin{bmatrix} x \\ \dot{x} \end{bmatrix}(t_k) + \begin{bmatrix} (t_{k+1} - t_k)^2/2 \\ t_{k+1} - t_k \end{bmatrix} \hat{\ddot{x}}(t_k|t_k) \tag{22}$$

Likewise for y and z directions.

This *state-dependent* piecewise-constant acceleration model is simple and straightforward for application. (22) is used for state prediction to get $\hat{\mathbf{x}}(t_{k+1}|t_k)$. For the propagation of the associated error covariance needed in, e.g., Kalman filtering, it is proposed in [18] to add, in effect, component-uncoupled small noise $\mathbf{w}(t_k) = [w_x, w_y, w_z]'(t_k)$ to $[\hat{\ddot{x}}, \hat{\ddot{y}}, \hat{\ddot{z}}]'(t_k|t_k)$ in the dynamics equation, where $\text{cov}(\mathbf{w}) = \text{diag}(q_x, q_y, q_z)$ is a design parameter. As a result, what is proposed is a coordinate-"uncoupled," state-dependent piecewise-constant nonzero-mean white-noise acceleration model, using the terminology of [20, 1]. There seems room for improvement here by a better way of adding noise or by adding temporally or spatially correlated noise, but at a price of increased complexity.

Note that the motions along x, y, and z directions described by this model are not actually uncoupled over a period of multiple time steps. The coupling arises from the dependence of the acceleration on the common target state in (21). This model has been reported in [18] to provide quite satisfactory performance — competitive with the EKF based on the fully coupled nonlinear inverse-square model — for several BT tracking scenarios with a high sampling rate (of 4 Hz).

We emphasize that the underlying idea of this approach is not restricted to coast models or the specific form of the acceleration model used: The piecewise-constant approximation can be directly applied in any situation where the total acceleration is available as a function of the position and velocity, such as those described in later sections. Its accuracy depends mainly on the sampling rate. Given the attractive simplicity and accuracy of this model, it seems worthwhile to try this model in conjunction with some more precise acceleration models, rather than (17) as originally proposed in [18].

3.4 Models in Other Coordinates

Models in other CSs (e.g., radar face CS and spherical CS) can be obtained by conversion from the ENU-CS. For example, an explicit expression of the inverse-square model (neglecting the Coriolis and centrifugal forces) can be found in [25].

4 Reentry

During the atmospheric reentry phase, two significant forces always act on the target: the Earth's *gravity* and atmospheric *drag*. If maneuvers are possibly present, a third force — aerodynamic *lift* force — must also be considered. A reentry vehicle (RV) is referred to as a maneuvering RV (MaRV) if it involves maneuvers or ballistic RV (BRV) if it does not.

Formally the total acceleration of an RV is given by (2) or (3) with a zero thrust acceleration term ($\mathbf{a}_T = 0$). Most RV motion models can be viewed as coast models plus additional but dominating terms to account for drag and possibly lift. In fact, during reentry aerodynamic forces (drag and possibly lift) are usually much greater than gravity: drag in excess of $20g$ can be present over most of the RV trajectory below 30 km, possibly as high as $100g$, and lift and other transverse loads can easily exceed $10g$. Also, the effect of the Coriolis and centrifugal forces and the Earth oblateness on the target motion is much smaller than during the coast flight.

We first describe the models for drag and lift, and then present models for the motion of a BRV and MaRV respectively. Note that [26] is a useful reference but is largely overlooked by the tracking community so far.

4.1 Aerodynamic Forces

Drag. The drag force acts opposite to the target velocity vector $\mathbf{v}_r$, *relative to the atmosphere (*e.g., as seen in the ENU-CS or ECF-CS rather than the ECI-CS), with a magnitude proportional to the air density ρ and the square of the target speed v_r. Specifically, the drag induced acceleration is given by [3]

$$\mathbf{a}_D = -\frac{1}{2}\alpha\rho(h)\, v_r^2 \mathbf{u}_v \quad \text{for} \quad \mathbf{u}_v = \frac{1}{v_r}\mathbf{v}_r \tag{23}$$

where ρ is the air density, h denotes the target altitude, and α is referred to as *drag parameter*, given by $\alpha = Sc_D/m$ through the target mass m, the reference area S (defined as the target body cross-sectional area perpendicular to the velocity), and the so-called drag coefficient c_D. The coefficient c_D generally depends on S and $\mathbf{v}$, but is sometimes assumed constant [9]. The inverse of the drag parameter $\beta = 1/\alpha$ is known as the *ballistic coefficient* (BC). Consequently, for the tracking purpose, all uncertainties associated with the drag (other than the air density and velocity) are generally aggregated in (the dynamic models of) the drag parameter α (or equivalently the ballistic coefficient β) within the simple drag formulation (23).

Lift. The lift force on an RV can be any direction in the plane perpendicular to the velocity vector [26]. The presence of a lift force causes also a change in the target ballistic profile, which is accounted for by an additional drag, referred to as a *residual* or *induced* drag, acting along the negative velocity direction. Like the zero-lift drag, both lift and its induced drag have a magnitude proportional to $\frac{1}{2}\rho(h)\, v_r^2$. This factor quantifies the free-stream dynamic pressure [3] and is indispensable in the RV dynamic models.

The *complete* aerodynamic acceleration is the vector sum of drag and lift:

$$\mathbf{a}_A = \mathbf{a}_D + \mathbf{a}_D^{(r)} + \mathbf{a}_L \tag{24}$$

where $\mathbf{a}_D$ is the zero-lift drag component, given by (23), $\mathbf{a}_D^{(r)}$ is the residual (lift induced) drag, and $\mathbf{a}_L$ is the lift acceleration, perpendicular to the velocity vector.

Air Density. The air density ρ needed in the above models is usually approximated as an exponential function [27, 26, 28] or more accurately as a *locally* exponential function[8] of the target altitude [6, 29, 30]:

$$\rho(h) = \rho_0 e^{-\kappa h} \tag{25}$$

where ρ_0 and κ are known constants. See, e.g., [30] for the parameters of the local exponential functions. More precise but nonanalytic models of the air density are available [26].

4.2 Ballistic (Nonmaneuvering) RV Motion

In simple terms, a nonmaneuvering reentry vehicle travels along a "purely" ballistic trajectory in the atmosphere, hence the name *ballistic* RV (BRV). Such an endo-atmospheric motion is governed by atmospheric drag, the Earth's gravity, and depending on the CS, the Coriolis and centrifugal forces.

Knowing the important role the drag parameter plays in the drag, it should come as no surprise that BRV motion models can be classified into two groups: with and without knowledge of the drag parameter.

4.2.1 Kinematic Models (Known Drag Parameter)

If the drag parameter α (or the BC β) is (assumed) known, obtaining motion models of a BRV is straightforward by using a coast models of Sec. 3 and an additional drag model (23). Since the drag is a function of the *relative* velocity, it is more convenient to use some Earth-fixed CS (usually the ENU-CS), instead of the ECI-CS.

Consider first the simplest case. Assuming a flat, nonrotating Earth model with a constant gravity [9] (i.e., neglecting the Coriolis and centrifugal accelerations and treating the target as a mass-point with constant mass), it follows directly from (23)

[8] "Local" in the sense that the function is piecewise exponential, with parameters depending on the target height; that is, each piece corresponds to some layer of the atmosphere.

[9] This could be acceptable for low-altitude targets.

with (25) that a BRV motion model has the following state-space form in the sensor ENU-CS [31, 29, 28]:

$$\begin{bmatrix} \ddot{x} \\ \ddot{y} \\ \ddot{z} \end{bmatrix} = - \begin{bmatrix} 0 \\ 0 \\ g \end{bmatrix} - \frac{1}{2}\alpha\rho_0 e^{-\kappa z}\sqrt{\dot{x}^2+\dot{y}^2+\dot{z}^2} \begin{bmatrix} \dot{x} \\ \dot{y} \\ \dot{z} \end{bmatrix} \tag{26}$$

The complete model for the six-state vector $\mathbf{x} = (x, y, z, \dot{x}, \dot{y}, \dot{z})'$ is cast in an obvious manner. Note that $h = z$ in this case. Usually model noise is also introduced in (26), but for brevity we will omit it. Its covariance is a design parameter. The state vectors in such a *kinematic* model involves only the kinematic variables of the RV, hence the name.

A more accurate model is obtained if the above flat Earth model is replaced by a better Earth model. Two such more accurate models in the ENU-CS, with the spherical and ellipsoidal Earth models, respectively, are given by

$$\begin{bmatrix} \ddot{x} \\ \ddot{y} \\ \ddot{z} \end{bmatrix} = \mathbf{g}_i(\mathbf{x}) - \frac{1}{2}\alpha\rho_0 e^{-\kappa h}\sqrt{\dot{x}^2+\dot{y}^2+\dot{z}^2} \begin{bmatrix} \dot{x} \\ \dot{y} \\ \dot{z} \end{bmatrix} \tag{27}$$

where $\mathbf{g}_i(\mathbf{x})$ for $i = 1, 2$ were defined in coast models (17) and (18) for spherical and ellipsoidal Earth models, respectively. While for the spherical model ($i = 1$) in (27) the target height $h = z$, for the ellipsoidal model ($i = 2$) h can be approximated by the distance between the target position and the intersection point of the vector $\mathbf{p}$ with the reference ellipsoid (Fig. 1**)** [24]. More details of the ellipsoidal Earth based model (27), along with the calculation of the Jacobian and the successive transformations to the radar face and RUV-CS, can be found in [11]. For an analysis of this model in the radar face CS, the reader is referred to [32, 6].

Conceptually a motion model in the Cartesian CS is most natural. In the RV tracking, however, actual measurements of a dish or phased array radar are typically expressed in some other CS, such as the spherical or RUV CS. These measurements have a highly nonlinear relationship with the target state variables in the Cartesian CS. Often EKF-based nonlinear filtering techniques [6, 11] are employed to handle both dynamics and measurement nonlinearities. This can be done in a mixed coordinate system — the state vector in the Cartesian CS and measurements in the sensor CS. Alternatively, either the measurements can be converted to the Cartesian CS or the state can be converted to the sensor CS. As remarked in [33], measurement conversion, along with proper initialization and prediction, yields tracking performance comparable to state conversion. The study reported in [6] concludes that in the normal circumstances, the measurement nonlinearities play a more important role than the dynamics nonlinearities. Along this line, it was argued in [29] that modeling the RV motion in the sensor CS rather than the Cartesian CS could be advantageous. A BRV motion model assuming an ellipsoidal Earth is used in the spherical CS of a dish radar in [24]. While the motion model is too lengthy to be included here, the measurement model is the simplest possible. It allows one to circumvent such critical issues as linearization of the measurement model and CS conversions. On the basis of it, as reported in [24], a practical system for tracking incoming ballistic targets was successfully implemented. For a complete coverage of this topic, the reader is referred to Part III [2].

A first-order Markov (Singer) model for the target acceleration is used in [34], where the correlation parameter is linked to the dynamic pressure along the target trajectory.

4.2.2 Dynamic Models (Unknown Drag Parameter)

The assumption of a known drag parameter α (or β) greatly simplifies the modeling of the RV motion. However, it is usually not valid in practice — the drag parameter is unknown and needs to be estimated. The prevailing approach to handling this extra uncertainty is by state augmentation: augment the kinematic state vector of an RV by some time-varying parameters used to model the drag parameter. The dynamics equation of these parameters, together with a kinematic model as given above, thus forms a *dynamic* model of the RV.

Probably the simplest model[10] is to augment the RV kinematic state vector by the drag parameter itself in, e.g., the Cartesian coordinates as $\mathbf{x}_a = [x, y, z, \dot{x}, \dot{y}, \dot{z}, \alpha]'$ and assume an unknown but (nearly) constant drag parameter $\alpha(t)$; that is, model $\alpha(t)$ as a Wiener (or more generally independent increment) random process governed by

$$\dot{\alpha} = w_\alpha(t) \tag{28}$$

where $w_\alpha(t)$ is zero-mean white noise. Then a complete RV dynamic model is obtained by concatenating (28) with some RV kinematic model, e.g., (26) or (27). This simple drag model is probably the most common in the BRV tracking literature. It was used in combination with various RV kinematic models in [32, 6, 31, 24]. The variance of w_α is a design parameter.

[10] If we do not consider using a priori drag tables [24].

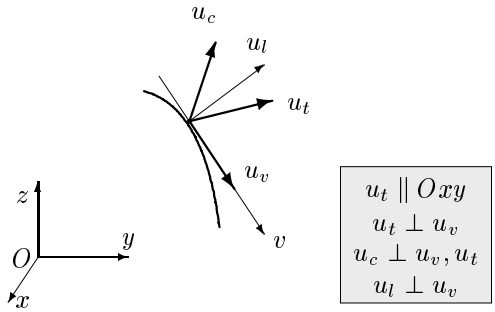

Fig. 2: Maneuvering RV Model

In reality the drag parameter α is not constant — it is an (unknown) function of the target altitude h and speed. Assuming an exponential air-density model (25) with a fixed set of ρ_0 and κ, the ballistic coefficient β is approximated in [29] as a linear function of the height z: $\beta = \beta_0 + \beta_1 z$, where β_0 and β_1 are unknown parameters, incorporated into the state vector to be estimated. This linear model, however, turns out to be quite inaccurate over some altitude ranges. As an enhancement, it was proposed further in [29] to introduce a new variable $\gamma \triangleq \rho/\beta = \alpha\rho$ with a dynamics equation $\dot{\gamma} = -\kappa\gamma(t)\,\dot{z}(t)$ based on the locally exponential model of ρ (25), where κ is a constant, specified over several altitude ranges. More specifically, the resulting *dynamic* BRV model — based on, e.g., the kinematic model (26) with a flat Earth model — becomes:

$$\begin{bmatrix} \ddot{x} \\ \ddot{y} \\ \ddot{z} \end{bmatrix} = -\frac{1}{2}\gamma\sqrt{\dot{x}^2+\dot{y}^2+\dot{z}^2}\begin{bmatrix} \dot{x} \\ \dot{y} \\ \dot{z} \end{bmatrix} - \begin{bmatrix} 0 \\ 0 \\ g \end{bmatrix} \tag{29}$$

$$\dot{\gamma} = -\kappa\gamma\dot{z} \tag{30}$$

In this model, κ is a key parameter, also unknown. Its uncertainty is handled in [29] by means of an *interval* Kalman filtering technique developed recently, assuming κ is in a known interval of a length $2\Delta_\kappa$ center at a nominal value κ_0.

Another idea to model the drag parameter is to consider its deviation from an a priori known, *nominal* value $\overline{\alpha}$ in terms of the ratio $\alpha/\overline{\alpha}$ [11]. Assuming its logarithm $\delta \triangleq \ln(\alpha/\overline{\alpha})$ is constant (i.e., $\dot{\alpha}/\alpha = 0$ with $\alpha = \overline{\alpha}e^{\delta}$), an RV kinematic model can be augmented with the model $d\delta/dt = 0$ in an obvious manner. In [11] this is done for (27) with the ellipsoidal Earth model. In our opinion, it seems more effective to assume $\dot{\delta}(t) = w_\delta(t)$ with white noise $w_\delta(t)$ or model $\delta(t)$ as a first-order Markov process (i.e., a Singer model). Note that the use of a fixed nominal value $\overline{\alpha}$ makes the model practically applicable only for a known *class* of targets with α corresponding to the chosen $\overline{\alpha}$. The uncertainty associated with the drag is a rather complex issue, analyzed in great detail in [26].

4.3 Maneuvering RV Motion

An important feature of the above models involving a known or unknown drag parameter is that they account for the drag effects along the velocity vector only (i.e., along the ballistic trajectory of an RV). For an maneuvering RV (MaRV), accounting for possible lift and residual drag requires introducing also a lateral acceleration model into the complete aerodynamic acceleration.

4.3.1 Models of Aerodynamic Forces

The magnitudes of the lift and its induced drag are given above. A more detailed model of the aerodynamic forces, including both drag and lift, involves expressing the lift and the induced drag in an appropriate coordinate system.

Models in Body Frame. The lift may be decomposed into two components for convenience (see Fig. 2) [31, 35]: *turn* force (along unit vector $\mathbf{u}_t$) and *climb* force (along unit vector $\mathbf{u}_c$). The turn direction $\mathbf{u}_t$ is horizontal[11] and perpendicular to the velocity vector (i.e., $\mathbf{u}_t \parallel Oxy$ and $\mathbf{u}_t \perp \mathbf{u}_v$), and the climb direction $\mathbf{u}_c$ is perpendicular to the turn and velocity vectors

[11] Although a flat Earth model is assumed in [31], $\mathbf{u}_t$ can be thought of as tangential to the reference ellipsoid in an ellipsoidal Earth model, i.e., $\mathbf{u} \parallel Oxy$ in the ENU-CS.

(i.e., $\mathbf{u}_c \perp \mathbf{u}_t$ and $\mathbf{u}_c \perp \mathbf{u}_v$). Formally $\mathbf{u}_t \triangleq \mathbf{u}_z \times \mathbf{u}_v$ and $\mathbf{u}_c \triangleq \mathbf{u}_v \times \mathbf{u}_t$, where $\mathbf{u}_z = [0,0,1]'$ is the unit vertical vector. The triple of unit vectors $\mathbf{u}_v$, $\mathbf{u}_t$, $\mathbf{u}_c$ defines an orthogonal CS, centered at the target position, which we will loosely refer to as a *"body frame"* (BF)[12]. Then analogically to (23), it follows from (24) that the complete aerodynamic acceleration $\mathbf{a}_A$ is expressed in the BF as

$$\mathbf{a}_A = \frac{1}{2}\rho v^2 \boldsymbol{\alpha} = \frac{1}{2}\rho v^2 \left(-\alpha_d \mathbf{u}_v + \alpha_t \mathbf{u}_t + \alpha_c \mathbf{u}_c\right) = \frac{1}{2}\rho v^2 \left[\mathbf{u}_v, \mathbf{u}_t, \mathbf{u}_c\right] \begin{bmatrix} -\alpha_d \\ \alpha_t \\ \alpha_c \end{bmatrix} \tag{31}$$

where $\alpha_d = \left(1+\lambda^2\right)\alpha$. The parameters α_t and α_c quantify the lift along the horizontal turn and climb directions, respectively. The parameter λ — the ratio of the lift to the critical lift (i.e., the lift at the maximum lift-to-drag ratio) — characterizes the residual drag parameter in terms of the basic, zero-lift drag parameter α as $\lambda^2\alpha$. After conversion to the ENU-CS[13] we have

$$\mathbf{a}_A = \frac{1}{2}\rho v^2 T_{\text{BF}}^{\text{ENU}}(\mathbf{v}) \begin{bmatrix} -\alpha_d \\ \alpha_t \\ \alpha_c \end{bmatrix} \tag{32}$$

The BF-to-ENU coordinate transformation matrix $T_{\text{BF}}^{\text{ENU}}$ can be given in two alternative forms:

$$T_{\text{BF}}^{\text{ENU}}(\mathbf{v}) = \begin{bmatrix} \dot{x}/v & -\dot{y}/v_g & -\dot{x}\dot{z}/(vv_g) \\ \dot{y}/v & \dot{x}/v_g & -\dot{y}\dot{z}/(vv_g) \\ \dot{z}/v & 0 & v_g^2/(vv_g) \end{bmatrix} \tag{33}$$

$$T_{\text{BF}}^{\text{ENU}}(\theta,\,\phi) = \begin{bmatrix} \cos\theta\cos\phi & -\cos\phi & \sin\theta\cos\phi \\ \cos\theta\sin\phi & \sin\phi & \sin\theta\sin\phi \\ -\sin\theta & 0 & \cos\theta \end{bmatrix} \tag{34}$$

where $v = \sqrt{\dot{x}^2+\dot{y}^2+\dot{z}^2}$ and $v_g = \sqrt{\dot{x}^2+\dot{y}^2}$ are the target speed and ground speed, respectively, and $\phi = \tan^{-1}(\dot{y}/\dot{x})$ and $\theta = \tan^{-1}\left(-\dot{z}/\sqrt{\dot{x}^2+\dot{y}^2}\right)$ are the *velocity* "heading" and "elevation" angles respectively.

This model allows a simple physical interpretation: $\alpha_t > 0$ (or $\alpha_t < 0$) corresponds to a left (or right) ground turn, while $\alpha_c > 0$ (or $\alpha_c < 0$) corresponds to climbing up (or diving). Such a clear interpretation could facilitate the adjustment of the model parameters and RV tracking by multiple models, among other things. An MaRV aerodynamic model so specified requires in general four parameters: α, λ, α_t, and α_t. Clearly, as pointed out in [31], not all these parameters are observable since (31) depends on them only through three scalar parameters: α_d, α_t, and α_c. Thus, loosely speaking we can consider $\boldsymbol{\alpha} = [-\alpha_d, \alpha_t, \alpha_c]'$ as a parameter vector characterizing maneuvers of an MaRV, although α_d is actually dominated by the nonmaneuvering zero-lift drag.

A similar model in the aerodynamic frame was presented in [26] based on a zero-lift nominal trajectory, which has an 8-dimensional state vector involving the lift parameters $\boldsymbol{\alpha} = -[\alpha_t, \alpha_c]'$ as well as the kinematic variables.

Models in LOS-CS. Alternatively, the residual drag $\mathbf{a}_D^{(r)}$ and lift acceleration $\mathbf{a}_L$ in (24) can be expressed [11] in the following line-of-sight (LOS) coordinate system defined by the unit vectors $\mathbf{u}_\xi = \mathbf{r}/\|\mathbf{r}\|, \mathbf{u}_\eta = \mathbf{h}\times\mathbf{r}/\|\mathbf{h}\times\mathbf{r}\|$, and $\mathbf{u}_\zeta \triangleq \mathbf{u}_\xi \times \mathbf{u}_\eta$, where $\mathbf{h} = (\mathbf{r}+\boldsymbol{\rho})\times\mathbf{v}$. Here the ξ-axis is along the position vector in the ENU-CS, the η-axis is along the angular momentum vector, and the ζ-axis is determined by the right-hand rule. Denote the vector sum $\tilde{\boldsymbol{\alpha}}$ of the lift and the residual drag in this LOS-CS as $\tilde{\boldsymbol{\alpha}} = \alpha_\xi \mathbf{u}_\xi + \alpha_\eta \mathbf{u}_\eta + \alpha_\zeta \mathbf{u}_\zeta$. It is thus clear that the parametric vector $\tilde{\boldsymbol{\alpha}} = [\alpha_\xi,\, \alpha_\eta,\, \alpha_\zeta]'$ quantifies the maneuvers of an MaRV in the LOS-CS. After conversion to the ENU-CS the total aerodynamic acceleration is [11]

$$\mathbf{a}_A = \frac{1}{2}\rho v^2 \overline{\alpha}\left(-\frac{1}{v}\begin{bmatrix}\dot{x}\\ \dot{y}\\ \dot{z}\end{bmatrix} + T_{\text{LOS}}^{\text{ENU}}(\mathbf{x})\begin{bmatrix}\alpha_\xi\\ \alpha_\eta\\ \alpha_\zeta\end{bmatrix}\right) \tag{35}$$

where $\overline{\alpha}$ is a nominal value of the zero-lift drag parameter, discussed before, and

$$T_{\text{LOS}}^{\text{ENU}}(\mathbf{x}) = \left[\mathbf{u}_\xi(\mathbf{x}), \mathbf{u}_\eta(\mathbf{x}), \mathbf{u}_\zeta(\mathbf{x})\right] \tag{36}$$

is the LOS-to-ENU coordinate transformation matrix, determined by evaluating $\mathbf{u}_\xi$, $\mathbf{u}_\eta$, $\mathbf{u}_\zeta$ in terms of the kinematic state vector $\mathbf{x}$ in the ENU-CS. Detailed information can be found in [11].

[12] [26] uses a similar coordinate system, called an aerodynamic frame, which has only different axial orientation from the BF.

[13] That is, evaluate $T = [\mathbf{u}_v, \mathbf{u}_t, \mathbf{u}_c]$ in the ENU-CS: $\mathbf{u}_v = [\dot{x},\dot{y},\dot{z}]'/v, \mathbf{u}_t = [0,0,1]'\times\mathbf{u}_v = [-\dot{y},\dot{x},0]'/v_g, \mathbf{u}_c = \mathbf{u}_v\times\mathbf{u}_t = [-\dot{x}\dot{z}, -\dot{y}\dot{z}, \dot{x}^2+\dot{y}^2]'/(vv_g)$

Discussion. Although the above two models are conceptually similar, there are two main differences. First, the model in the BF avoids the unobservability problem by lumping the drag and lift-induced drag, while the LOS-CS model accomplishes this by the use of a nominal value $\overline{\alpha}$ for the zero-lift drag parameter. They are theoretically equivalent for the pure lift part. For the drag part, the latter amounts to estimating its variation relative to the nominal value, while the former to estimating the total drag. The latter model should be better in the case where this nominal $\overline{\alpha}$ is known (approximately), as in the case of a known RV type. Sometimes α is assumed constant because it usually does not change much over a wide range of altitude [26]. The other main difference lies in the choice of CS to parameterize the lift and residual drag. In general, the use of the observer-dependent LOS-CS for parameterization of target maneuver is more convenient from the observer (sensor) point of view, but it gives rise to a dependence of the maneuver parameters on the specific observer-target geometry, with some undesirable consequences. These include, among other things, an increased complexity of adjusting design parameters. In contrast, the BF representation depends on the target-Earth geometry only and is invariant of the sensor location. Furthermore, in the BF the lift (responsible for maneuvers) lies always in its y-z plane, while the nonmaneuvering force (i.e., the drag) is always along the x-axis. Such a decomposition makes the tracking task relatively easier. In this aspect a BF parameterization is probably preferable. As far as error coupling and ill conditioning are concerned, while the BF is good in terms of process error decoupling, LOS-CS is better regarding measurement error decoupling [7]. In this regard, it appears that the range-velocity Cartesian coordinates (RVCC) [7] should be considered. Consequently, if a reasonably good nominal value $\bar{\alpha}$ is available, we recommend the use of the following model

$$\mathbf{a}_A = \frac{1}{2}\rho v^2 \overline{\alpha} \left(-\frac{1}{v} \begin{bmatrix} \dot{x} \\ \dot{y} \\ \dot{z} \end{bmatrix} + T_{\text{RVCC}}^{\text{ENU}}(\mathbf{v}) \begin{bmatrix} \alpha_x' \\ \alpha_y' \\ \alpha_z' \end{bmatrix} \right) \tag{37}$$

4.3.2 Motion Models

Given models of the aerodynamic acceleration in the ENU-CS, development of a complete motion model of an MaRV is straightforward. One needs to choose a coast model, depending on the underlying assumptions concerning gravity (e.g., models with a flat, spherical, or ellipsoidal Earth), and then incorporate into it an aerodynamic acceleration model, such as (32) or (35) in the ENU-CS. This can also be done in the ECI-CS, in which case the aerodynamic acceleration $\mathbf{a}_A$ to be incorporated must be transformed to the ECI-CS. Such a model involves maneuver governing parameters, such as $\boldsymbol{\alpha} = [-\alpha_d, \alpha_t, \alpha_c]'$ if (32) is used or $\boldsymbol{\alpha} = [\alpha_\xi, \alpha_\eta, \alpha_\zeta]'$ if (35) is used. These parameters are unknown and thus to be estimated. As for the dynamic BRV models, the state augmentation is commonly used: augment the kinematic state vector $\mathbf{x} = [x, y, z, \dot{x}, \dot{y}, \dot{z}]'$ by the unknown parameters (i.e., $\mathbf{x}_{\boldsymbol{\alpha}} \triangleq [\mathbf{x}', \boldsymbol{\alpha}']'$). Thus a dynamic model for $\boldsymbol{\alpha}$ is needed. Various models are possible here, although only a few have been proposed explicitly.

Wiener Process Models. The simplest possible model for $\boldsymbol{\alpha}$ is to assume it is "nearly constant": for example, model $\boldsymbol{\alpha}$ as a Wiener (or independent increment) random process governed by [31]

$$\dot{\boldsymbol{\alpha}} = \mathbf{w}_{\boldsymbol{\alpha}}(t) \tag{38}$$

where $\mathbf{w}_{\boldsymbol{\alpha}}(t)$ is zero-mean white noise. Such an MaRV model, based on (38) and a flat Earth model for the gravity, was proposed and investigated in [31] and in our notation can be compactly given in the ENU-CS as

$$\begin{bmatrix} \ddot{x} \\ \ddot{y} \\ \ddot{z} \end{bmatrix} = \mathbf{g}_0 + \frac{1}{2}\rho v^2 T_{\text{BF}}^{\text{ENU}}(\mathbf{v}) \begin{bmatrix} -\alpha_d \\ \alpha_t \\ \alpha_c \end{bmatrix} + \mathbf{w}(t) \tag{39}$$

$$\dot{\boldsymbol{\alpha}} = \mathbf{w}_{\boldsymbol{\alpha}}(t) \tag{40}$$

with $\boldsymbol{\alpha} = [-\alpha_d, \alpha_t, \alpha_c]'$, where $\mathbf{w}(t)$ is small white noise, $\mathbf{g}_0 = [0, 0, -g]'$ is the Earth's constant gravity vector and $T_{\text{BF}}^{\text{ENU}}(\mathbf{v})$ is given by (33). It clearly reduces to the nearly-constant-drag seven-state BRV model [31] with $\alpha_t = 0$ and $\alpha_c = 0$.

For better accuracy, the above flat, nonrotating Earth model can be replaced by a more sophisticated one, such as a spherical or ellipsoidal Earth model; that is, $\mathbf{g}_0$ in the above can be replaced with $\mathbf{g}_1(\mathbf{x})$ of (17) or $\mathbf{g}_2(\mathbf{x})$ of (18). These models expressed in the ENU-CS are somewhat more complicated due to the Coriolis and centrifugal terms than in the ECI-CS, which, however, requires the ENU-to-ECI coordinate transformation for the aerodynamic acceleration. Such a model

with $\boldsymbol{\alpha} = [-\alpha_d,\, \alpha_t,\, \alpha_c]'$ of (32) was developed and used in [16, 5]

$$\begin{bmatrix} \ddot{x} \\ \ddot{y} \\ \ddot{z} \end{bmatrix} = -\frac{\mu}{p^3}\begin{bmatrix} x \\ y \\ z \end{bmatrix} + \frac{1}{2}\rho v^2 T_{\text{ENU}}^{\text{ECI}} T_{\text{BF}}^{\text{ENU}} \begin{bmatrix} -\alpha_d \\ \alpha_t \\ \alpha_c \end{bmatrix} + \mathbf{w}\,(t) \tag{41}$$

$$\dot{\boldsymbol{\alpha}} = \mathbf{w}_{\boldsymbol{\alpha}}\,(t) \tag{42}$$

where $\mathbf{w}\,(t)$ is small white noise, $T_{\text{ENU}}^{\text{ECI}}$ is the ENU-to-ECI coordinate transformation [10]. Note that x, y, z, p, v are in the ECI-CS here. Obviously, the more accurate model (10) in the ECI-CS could be used for the gravity part instead.

For further information or relevant issues of this class of models, such as adjustment and possibly adaptation of the design parameters [e.g., the process noise matrix $Q = \text{cov}(\mathbf{w})$] and performance results, the reader is referred to [31, 35, 16, 5].

Markov Models. Alternatively and slightly more sophisticated, $\boldsymbol{\alpha}$ can be modeled as a first-order Markov process (as the Singer model for aircraft maneuvers):

$$\dot{\boldsymbol{\alpha}} = -K\boldsymbol{\alpha}\,(t) + \mathbf{w}_{\boldsymbol{\alpha}}\,(t) \tag{43}$$

where $\mathbf{w}_{\boldsymbol{\alpha}}\,(t)$ is zero-mean white noise and K is determined by design. If $\boldsymbol{\alpha}$ is associated with a *single* physical acceleration, K should be a scalar, otherwise it can be a (diagonal) matrix. Such a model was proposed in [11] for the maneuver governing parameters $\boldsymbol{\alpha} = [\alpha_\xi, \alpha_\eta, \alpha_\zeta]'$ of (35) in the ENU-CS[14], with $K = \text{diag}(\kappa_\xi, \kappa_\eta, \kappa_\zeta)$ (for $\kappa_\eta = \kappa_\zeta$)

$$\begin{bmatrix} \ddot{x} \\ \ddot{y} \\ \ddot{z} \end{bmatrix} = \mathbf{g}_2\,(\mathbf{x}) - \frac{1}{2}\rho v^2 \overline{\alpha}\left(\frac{1}{v}\begin{bmatrix} \dot{x} \\ \dot{y} \\ \dot{z} \end{bmatrix} - T_{\text{LOS}}^{\text{ENU}}\,(\mathbf{x})\begin{bmatrix} \alpha_\xi \\ \alpha_\eta \\ \alpha_\zeta \end{bmatrix}\right) + \mathbf{w}\,(t) \tag{44}$$

$$\dot{\boldsymbol{\alpha}} = -K\boldsymbol{\alpha}\,(t) + \mathbf{w}_{\boldsymbol{\alpha}}\,(t) \tag{45}$$

where $\mathbf{w}\,(t)$ is small white noise, $\mathbf{g}_2\,(\mathbf{x})$ is given in (18), and $T_{\text{LOS}}^{\text{ENU}}\,(\mathbf{x})$ is defined by (36). To our knowledge this is the most comprehensive dynamic model for MaRV tracking used in the literature. It utilizes the "truly dynamic" first-order Markov model in conjunction with the highly accurate ellipsoidal Earth gravity model. Its (essentially) equivalent variants (e.g., in the ECI-CS) can be developed in an obvious manner. Similarly, the Singer model was adopted in [26] for the lift parameters $\boldsymbol{\alpha} = -[\alpha_t, \alpha_c]'$ in the aerodynamic frame.

Note that albeit conceptually the same, modeling $\boldsymbol{\alpha} = [-\alpha_d,\, \alpha_t,\, \alpha_c]'$ with (32) [31] and modeling $\boldsymbol{\alpha} = [\alpha_\xi, \alpha_\eta, \alpha_\zeta]'$ with (35) [11] as a white or Markov process are practically different (see the discussion in the previous subsection). Consequently, it is meaningful to develop and investigate a comprehensive dynamic model of an MaRV using $\boldsymbol{\alpha} = [-\alpha_d,\, \alpha_t,\, \alpha_c]'$, parallel to the above model with $\boldsymbol{\alpha} = [\alpha_\xi, \alpha_\eta, \alpha_\zeta]'$.

The above dynamics models of an MaRV relies on three ideas: (a) model the unknown aerodynamic acceleration through a parameter vector (scaled by a kinematic state-dependent factor $\frac{1}{2}\rho v^2$), (b) model this unknown (time-varying) parameter vector as a random process, and (c) augment the kinematic state vector with this parameter vector that quantifies maneuvers.

Unknown Input Models. Instead of modeling the uncertain drag and lift accelerations explicitly as above, their effects on the RV motion can be lumped and represented by an unknown input $\mathbf{u} = [u_x, u_y, u_z]'$ in the kinematic model of the MaRV: $\mathbf{a} = \mathbf{a}_D + \mathbf{g} + \mathbf{u}$ [36]. Specifically, with a flat Earth model, this new model takes the following form

$$\begin{bmatrix} \ddot{x} \\ \ddot{y} \\ \ddot{z} \end{bmatrix} = -\frac{1}{2}\alpha\rho\left(\dot{x}^2 + \dot{y}^2 + \dot{z}^2\right)\begin{bmatrix} \cos\theta\cos\phi \\ \cos\theta\sin\phi \\ -\sin\theta \end{bmatrix} - \begin{bmatrix} 0 \\ 0 \\ g \end{bmatrix} + \begin{bmatrix} u_x \\ u_y \\ u_z \end{bmatrix} + \begin{bmatrix} w_x \\ w_y \\ w_z \end{bmatrix} \tag{46}$$

which is a simple variation of (26) (i.e., with the addition of $\mathbf{u}$). Here the drag parameter α is assumed known, the drag acceleration is in a slightly different but clearly equivalent form in view of (34), and ϕ and θ are the *velocity* "heading" and (negative) "elevation" angles, respectively, as defined before.

This model is fairly ideal at first glance — the additional input $\mathbf{u}$ corresponds "exactly" to the acceleration (i.e., lift and its induced drag) responsible for the maneuvers. It is in fact idealistic because the drag parameter is not known in practice. In our opinion, the unknown drag parameter in the model is more reasonably replaced in practice by a (known) nominal value $\overline{\alpha}$,

[14] All driving noises are left out in [11].

although with this replacement any deviation from this nominal value will give rise to a nonzero term in the additional input and thus may trigger a state estimate correction in the input-estimation method as applied in [36].

The unknown input vector $\mathbf{u}$, as well as the kinematic state variables, is estimated in [36] by the well-known input-estimation method for adaptive filtering [37, 38]. While attractive for its apparent simplicity, the effectiveness, if not the applicability, of the input-estimation method here is more or less questionable due to its fundamental assumption that the unknown input is constant over the period of interest. In fact, the unknown input $\mathbf{u}$ is inherently time-varying and state dependent, as can be seen, e.g., from (35). Nevertheless, this is a simple model to which many adaptive filtering techniques effective for uncertain (time-varying) input can be applied.

As far as the maneuver-related accelerations are concerned, this unknown-input model can be loosely thought of as "nonparametric" (model-free) while the above drag parameter based models are "parametric" (i.e., model-based) in some sense. Their relative pros and cons are parallel to those of parametric and nonparametric models in general — the parametric ones are more preferable if reasonably good knowledge of the parameters involved is available, otherwise the nonparametric models may be considered.

5 Boost Phase

The boost phase of a rocket-powered BT target lasts from launch until the rocket's final stage burnout. During this phase, which is primarily endo-atmospheric, the target is subject to large thrust acceleration, as well as atmospheric drag and the Earth gravity. The thrust acceleration profiles[15] vary largely from one target to another, mainly depending on the target type. Indeed, while some targets maintain essentially constant thrust acceleration, others, multistage targets in particular, typically have an abruptly (jump-wise) changing thrust. Moreover, some more advanced targets can also have a considerably variable thrust during later stages [39, 9, 5].

5.1 Thrust

According to the Newtonian mechanics, the target thrust-induced acceleration is determined by the thrust magnitude T, target mass m, and unit vector $\mathbf{u}_T$ that specifies the thrust force direction as [4]

$$\mathbf{a}_T = \frac{T}{m}\mathbf{u}_T \tag{47}$$

The uncertainty associated with the thrust acceleration includes its magnitude $a_T = T/m$, and the thrust force direction $\mathbf{u}_T$, which in principle requires two angles to be well defined in the general case.

The total target acceleration during the boost phase, including thrust, drag, and gravity, is

$$\mathbf{a} = \mathbf{a}_T + \mathbf{a}_D + \mathbf{a}_G = \underbrace{\frac{T}{m}\mathbf{u}_T + \mathbf{a}_D}_{\mathbf{a}_N} - \frac{\mu}{p^3}\mathbf{p} \tag{48}$$

Of course, the last term above can be replaced by (5) for better accuracy. However, the thrust and drag are usually much larger than the gravity during the boost phase.

Ideally, it would be desirable to augment the kinematic state vector with the thrust *vector (*T and $\mathbf{u}_T$), drag magnitude $D = \frac{1}{2}\alpha\rho v^2$ (or equivalently the drag parameter α provided the air density ρ is known), and mass m so that they are estimated separately. However, *unobservability* problems would arise with such a state vector [9]. A more appropriate approach is to handle directly the *net* (thrust minus drag) acceleration $\mathbf{a}_N = \mathbf{a}_T + \mathbf{a}_D$ as defined in (48), rather than its components separately. This results in a 9-state vector $\mathbf{x} = (\mathbf{p}', \mathbf{v}', \mathbf{a}_N')'$. Of course, other forms of a state vector can be considered, such as in spherical coordinates with position (altitude, latitude, longitude), velocity (radial, northward, eastward), and thrust vector (magnitude, in-plane, out-of-plane directions of thrust direction), as used in [40]. In fact, one of the earliest reentry models has the state vector consisting of position in spherical coordinates (altitude, longitude, latitude), speed, heading angle (in the local horizon plane), and the flight path angle with respect to the local horizontal [13, 41].

[15] In this context, the acceleration magnitude and direction are functions of time.

5.2 Generic (Kinematic) Models

5.2.1 Constant Net-Acceleration Models

This model assumes a constant ($\dot{\mathbf{a}}_N = \mathbf{0}$) [15] or nearly constant ($\dot{\mathbf{a}}_N = \mathbf{w}$) [16] non-gravitational net acceleration. It is given by, with the 9-state vector $\mathbf{x} = (\mathbf{p}', \mathbf{v}', \mathbf{a}_N')'$,

$$\begin{aligned} \dot{\mathbf{p}} &= \mathbf{v} \\ \dot{\mathbf{v}} &= \mathbf{a}_N + \mathbf{a}_G \qquad (49) \\ \dot{\mathbf{a}}_N &= \mathbf{0} \quad \text{or} \quad \dot{\mathbf{a}}_N = \mathbf{w} \qquad (50) \end{aligned}$$

where $\mathbf{w}$ is "small" zero-mean white noise of a covariance that is treated as a design parameter.[16] It takes the simplest form in the ECI-CS, in which $\mathbf{p} = [x, y, z]'$, $\mathbf{a}_G$ is given by (4), (5), or $\mathbf{g}_0$, and $\mathbf{a}_N = [a_x, a_y, a_z]'$ (if $\mathbf{a}_N$ is expressed in the Cartesian coordinates) or $\mathbf{a}_N = a_N[\sin\theta_N \cos\phi_N, \sin\theta_N \sin\phi_N, \sin\theta_N]'$ (if $\mathbf{a}_N = [a_N,\ \phi_N,\ \theta_N]'$ is expressed in spherical coordinates through its magnitude a_N and angles ϕ_N and θ_N) [15].

The "nearly constant" version is suitable to cover small maneuvers for motions with a low level of thrust, and indeed was designed [16, 5] for a post-boost phase of motion, which is primarily exo-atmospheric with non-gravitational net acceleration on the order of 1 m/s^2.

Albeit conceptually equivalent to the ("nearly") constant-acceleration (CA) model for aircraft motion [1], this model is rather nonlinear due to the gravitational term $\mathbf{a}_G$ unless the constant gravity model $\mathbf{a}_G = \mathbf{g}_0$ is used. It assumes — in the absence of the gravitational effect — a 3D straight line motion with a constant acceleration. Further, this model allows in general a target motion with a non-zero *angle of attack*, defined as the angle between the thrust and velocity vectors, in contrast to the widely used *gravity turn* (GT) model, discussed later. As such, this model may be more appropriate than the GT model for tracking maneuvering (e.g., staging) BTs where the GT model's assumption is violated.

As explained in [1], a (nearly) CA model is in fact a second-order polynomial (i.e., quadratic) model. The motion is usually assumed uncoupled along the three dimensions [42] in a polynomial model. As reported in [39], however, such a quadratic model falls far short of the required accuracy in modeling even the entire first stage of a long-range target. Similar and simple models — a CA model with constant gravity in a multiple-model framework and second/third order polynomials — have been applied in [43, 44] for trajectory tracking and backfitting for launch point estimation.

5.2.2 Correlated Acceleration Models

The above model assumes that the net acceleration is constant or has an independent increment (or decrement). In reality, however, the net acceleration is dominated by the thrust, which has a strong temporal correlation. In such a case, although the above nearly-constant model can still be used with a larger noise at a cost of significantly deteriorated accuracy, it is certainly more appropriate to model the non-gravitational net acceleration as a first-order Markov process (i.e., the Singer model) [16] given by

$$\dot{\mathbf{a}}_N = -(1/\tau)\mathbf{a}_N + \mathbf{w} \qquad (51)$$

where $\mathbf{w}$ is zero-mean white noise. Not only the covariance of $\mathbf{w}$ but the correlation-time constant τ is also a design parameter now. Like before, due to the gravitational component in (49), the complete 9-state model is rather nonlinear.

Alternatively, the Singer model can be used directly for the *total*, rather than net, acceleration $\mathbf{a}$: $\dot{\mathbf{a}} = -(1/\tau)\mathbf{a} + \mathbf{w}$. This amounts to a Singer model for the gravity as well as the net acceleration and the resulting model with the complete 9-state vector $\mathbf{x} = (\mathbf{p}', \mathbf{v}', \mathbf{a}')'$ is linear. It is certainly less accurate than the above nonlinear 9-state model with the Singer model for the net acceleration due to the accuracy difference in the gravity models involved. Compared with the non-gravitational net acceleration, however, the gravitational acceleration is less significant during the boost phase. Both of these correlated acceleration models have demonstrated quite good performance for tracking boosting targets with real data, as reported in [5].

We emphasize that the models discussed in this entire subsection are fairly general; that is, they are not really flight phase specific — no information specific to the boost phase is utilized. Therefore, they are also applicable to the other two phases, but they cannot be expected to perform as well as good models specific for a flight phase.

5.3 Gravity-Turn Models

During the boost (post-boost) phase a ballistic target typically maintains a small angle of attack and thus approximately follows a trajectory known as a *gravity turn* (GT). A GT is characterized by the assumption that the thrust is parallel to the

[16] $\dot{\mathbf{a}}_N = \mathbf{w}$ implies that $\mathbf{a}_N$ is a Wiener process or more generally a random process with independent increments [1].

relative velocity vector [3], that is, parallel as seen by an observer in a coordinate system fixed to the Earth (e.g., the ECF-CS). Making use of this strong constraint can improve considerably modeling (and hence tracking) accuracy if the assumption is valid. This is in the same spirit as the kinematic constraint technique for, e.g., coordinated turns, discussed in [1].

5.3.1 Kinematic GT Models

A booster model that utilizes the GT assumption was proposed in [39]. It is a quadratic (second-order polynomial) model (see [1]) with a modification such that the acceleration and velocity vectors are parallel. Specifically, *in the ECF-CS* the state vector includes the kinematic components $(x, \dot{x}, y, \dot{y}, z, \dot{z})$ and possibly the ratio of the net acceleration magnitude to target speed, $\kappa \triangleq a/v$. As far as only non-gravitational net accelerations are concerned, the GT constraint reads as $\mathbf{a} = \kappa \mathbf{v}$ or

$$\ddot{x} = \kappa \dot{x}, \quad \ddot{y} = \kappa \dot{y} \quad , \ddot{z} = \kappa \dot{z} \tag{52}$$

The (nearly) constant net-acceleration (i.e., second-order polynomial) model subject to this GT constraint takes the following time-series form

$$\begin{bmatrix} x(t) \\ y(t) \\ z(t) \end{bmatrix} = \begin{bmatrix} a_0 & a_1 & \kappa a_1 \\ b_0 & b_1 & \kappa b_1 \\ c_0 & c_1 & \kappa c_1 \end{bmatrix} \begin{bmatrix} 1 \\ t - t_0 \\ (t - t_0)^2/2 \end{bmatrix} \tag{53}$$

where the model parameters to be estimated (i.e., $a_i, b_i, c_i,\ i = 0, 1$ and κ) are assumed time invariant. Note that $x,\ y,\ z$ are coupled only through κ. Many parameter estimation techniques, such as the least-squares (LS) method [39], can be used to estimate these parameters. In the case of an unknown κ, however, this is a nonlinear estimation problem, a simplified special case of which nevertheless has an exact LS solution, as given in [39]. Note that a_0, a_1, and κa_1 are actually position, velocity, and acceleration, respectively, along x-axis at time t_0 (likewise for y and z directions).

Although generally superior to the quadratic model of Sec. 5.2 for GT motions, this model appears to lack the accuracy required for more demanding tracking applications. As pointed out in [39], while performing well for constant thrust accelerations (typically valid only over short time periods), it is not generally adequate in the case of target staging (jump-wise changes of thrust acceleration). For such cases a generalization is suggested in [39]: augment the state vector with two additional angles (yaw and pitch) representing respectively the horizontal and vertical orientations of the acceleration vector relative to the velocity vector. This generalized model is in essence the quadratic model of Sec. 5.2 with $\mathbf{a}_N = [a_N, \phi_N, \theta_N]'$ expressed in spherical coordinates [15] subject to the GT constraint $a_N = \kappa v$.

The above GT models have been used in the time-series polynomial form. Its state-space form is given by [45]

$$\dot{\mathbf{x}} = \text{diag}[A, A, A]\mathbf{x} \quad \text{with} \quad A = \begin{bmatrix} 0 & 1 \\ 0 & \kappa \end{bmatrix} \tag{54}$$

where $\mathbf{x} = [x, \dot{x}, y, \dot{y}, z, \dot{z}]'$. Its usual discrete-time counterpart can be obtained as

$$\mathbf{x}_{k+1} = \text{diag}[F, F, F]\mathbf{x}_k \quad \text{with} \quad F = \begin{bmatrix} 1 & \frac{\exp(\kappa T) - 1}{\kappa} \\ 0 & \exp(\kappa T) \end{bmatrix} \tag{55}$$

assuming κ is piecewise constant (i.e., constant within any sampling period of length T). This model has only one parameter, κ, and is linear if κ is known or assumed known, such as in a multiple-model algorithm. Such a model is one of the simplest possible for the Kalman filtering. Therefore, this state-space form, albeit theoretically equivalent to the above polynomial form, appears to be superior for tracking purposes.

It is interesting to note the similarity and difference between a gravity turn (GT) and a coordinated turn (CT). Both motions are defined by kinematic constraints: While acceleration and velocity vectors are parallel ($\mathbf{a} \parallel \mathbf{v}$) in a GT, they are orthogonal ($\mathbf{a} \perp \mathbf{v}$) in a CT. The motions along the three dimensions are coupled in a GT only through $\kappa = |\mathbf{a}\|/\|\mathbf{v}\|$, and coupled in a CT only through the turn rate $\omega = |\mathbf{a}\|/\|\mathbf{v}\|$ (see (82)–(83) of [1]).

In the case where κ is not known, the above GT models are nonlinear and κ needs to be estimated. A "standard" technique for such a problem is state augmentation: Augment the state vector by κ where κ can be, for example, modeled as a Wiener process or a first-order Markov process, or modeled physically via flight dynamics of rocket-powered vehicles (see next subsubsection). Other adaptive modeling/estimation techniques may be applicable, particularly those proven effective for the coordinated turn motion, as discussed in great detail in Sections 5.1 and 5.2 of [1]. Other kinematic-constraint based techniques, such as pseudomeasurement based (see Sec. 6.4 of [2]), are applicable [45].

All the GT models discussed in this subsection account only for the non-gravitational net acceleration. In the absence of gravitational effects and with a constant κ, they clearly describe a 3D rectilinear motion with a constant acceleration. Use

of these models implicitly presumes that either the gravitational effects can be neglected or handled separately, such as by a correction of the target position offset (in sensor measurements) due to the gravity calculated at a nominal target altitude in [39].

5.3.2 Dynamic GT Models

The booster models discussed so far are essentially kinematic without the help of the knowledge about the flight dynamics specific for rocket-powered vehicles. However, there is no reason why rocket-specific dynamics cannot be utilized to develop more accurate models. These models are discussed next.

In a GT motion, the thrust, drag, and their net accelerations $\mathbf{a}_N$ are all parallel to the relative velocity vector $\mathbf{v}_r$ in an Earth fixed CS. For simplicity, let

$$\alpha \triangleq a_N = \frac{T-D}{m} \tag{56}$$

be the magnitude of the net acceleration, where T, D, and m are thrust, drag, and target mass, respectively. It thus follows that $\mathbf{a}_N = (\alpha/v_r)\mathbf{v}_r$, where $v_r = \|\mathbf{v}_r\|$ is the target speed.[17] In an Earth-fixed CS, this equation is then $[\ddot{x}, \ddot{y}, \ddot{z}]' = \frac{\alpha}{v_r}[\dot{x}, \dot{y}, \dot{z}]'$ with $v_r = \sqrt{\dot{x}^2 + \dot{y} + \dot{z}^2}$. In the ECI-CS, it becomes, after expressing $\mathbf{v}_r$ in the ECI-CS using (1),

$$[\ddot{x}, \ddot{y}, \ddot{z}]' = \frac{\alpha}{v_r}[\dot{x} - \omega_e y,\ \dot{y} + \omega_e x,\ \dot{z}]' \tag{57}$$

where ω_e is the Earth rotation rate and $v_r = \sqrt{(\dot{x} - \omega_e y)^2 + (\dot{y} + \omega_e x)^2 + \dot{z}^2}$. The unknown net acceleration α involved needs to be estimated. Its dynamics model is developed next.

It is often assumed that during the boost phase the thrust magnitude T is constant ($\dot{T} = 0$) and the target mass m is linearly decreasing (i.e., $\dot{m} + \delta_m = 0$) at a constant rate $\delta_m > 0$ [3]. Alternative to the assumption $\dot{T} = 0$, assume now that the magnitude of the non-gravitational net forces $F(t) \triangleq T(t) - D(t) = F(t_0)$ is constant,[18] where t_0 is an arbitrary initial time. Then we have, for $t \geq t_0$,

$$\alpha(t) = \frac{F(t)}{m(t)} = \frac{F(t_0)}{m(t_0) - \delta_m(t - t_0)} = \frac{\alpha(t_0)}{1 - \beta(t_0)(t - t_0)} \tag{58}$$

$$\beta(t) \triangleq \frac{\delta_m}{m(t)} = \frac{\delta_m}{m(t_0) - \delta_m(t - t_0)} = \frac{\beta(t_0)}{1 - \beta(t_0)(t - t_0)} \tag{59}$$

It follows from differentiating (58)–(59) that $\alpha(t)$ and $\beta(t)$ satisfy $\dot{\alpha} = \alpha(t)\beta(t)$ and $\dot{\beta} = \beta^2(t)$. Then the GT dynamics model in the ECI-CS follows from the total acceleration equation $\mathbf{a} = \mathbf{a}_N + \mathbf{a}_G = \alpha\frac{\mathbf{v}_r}{v_r} - \frac{\mu}{p^3}\mathbf{p}$, with the inverse-square model of gravity, and is given in the following state-space form [9]

$$\dot{\mathbf{p}} = \mathbf{v} \tag{60}$$

$$\begin{bmatrix} \ddot{x} \\ \ddot{y} \\ \ddot{z} \end{bmatrix} = \frac{\alpha}{v_r}\begin{bmatrix} \dot{x} - \omega_e y \\ \dot{y} + \omega_e x \\ \dot{z} \end{bmatrix} - \frac{\mu}{p^3}\begin{bmatrix} x \\ y \\ z \end{bmatrix} \tag{61}$$

$$\dot{\alpha} = \alpha(t)\beta(t) \tag{62}$$

$$\dot{\beta} = \beta^2(t) \tag{63}$$

for state vector $\mathbf{x} = [x,\ y,\ z,\ \dot{x},\ \dot{y},\ \dot{z},\ \alpha,\ \beta]'$.

This model is nonlinear. For state and covariance propagation, numerical integration by the Runge-Kutta method and linearization were used in [9]. Not only is this computationally inefficient, but it also inevitably injects possibly considerable errors, especially those associated with linearization. For enhancement, an extension of this 8-state GT model to a more general booster model is also reported in [9]. As in [15, 39], two additional angles (yaw and pitch), representing respectively the horizontal and vertical orientations of the acceleration vector with respect to the velocity vector, are incorporated into the state vector.

[17] Clearly, $\kappa = \alpha/v_r$ is the acceleration to velocity ratio, discussed above.

[18] This differs from [9], which in effect assumes that the drag acceleration $a_D = \frac{1}{2m}Sc_D\rho(h)v_r^2$ can be written in the form of (58).

As an alternative, we propose the following [45]. Note first that the continuous-time model (58)–(59) [or equivalently, (62)–(63)] of α and β has the following *exactly equivalent* discrete-time model

$$\alpha_{k+1} = \frac{\alpha_k}{1-\beta_k T} \tag{64}$$

$$\beta_{k+1} = \frac{\beta_k}{1-\beta_k T} \tag{65}$$

where $T = t_{k+1} - t_k$ is the sampling interval. Thus, state prediction for α and β can be done *precisely* (under the stated assumptions) in discrete time directly. Then the prediction of the kinematic components can be done by solving (61). This eliminates the need for the numerical integration to deal with the nonlinearity of α and β. Note that when additional noise is added, (62)–(63) and (64)–(65) are not generally equivalent. Also, which discrete-time value of α and β should be used for (61)? For a discussion of a similar situation, the reader is referred to Sec. 5.2 of [1].

A similar model was used in [19] (p. 138), where the net-acceleration model is directly specified by

$$\dot{\alpha} = \frac{1}{c}\alpha^2(t) \tag{66}$$

with an assumed known initial state $\alpha(t_0)$ and *known* constant c, representing exhaust velocity. [46] gives a derivation of the following more general model

$$\dot{\alpha} = \frac{1}{c}\alpha^2(t) + \frac{\ddot{m}}{\dot{m}}\alpha \tag{67}$$

which simplifies to (66) under the assumption $\ddot{m} = 0$.

Interestingly, it can be shown that for $c = F(t_0)/\delta_m = \alpha(t_0)/\beta(t_0)$ the *only* solution of (66) is exactly given by (58); that is, both models describe the same net acceleration and are thus theoretically equivalent with this c value. In practice, however, the model (66) is probably worse because it presumes knowledge of parameter c, which is in effect estimated in the former model. The exact discrete-time equivalent of (66) can be found for any given c to be

$$\alpha_{k+1} = \frac{\alpha_k}{1-\alpha_k T/c} \tag{68}$$

Other similar models for GT trajectory can be found in [47] and [48].

Note the difference between the kinematic GT models of Sec. 5.3.1 and the dynamic GT models here: While the key GT parameter α is modeled explicitly based on rocket dynamics in the latter, such a parameter, κ, is either assumed known or modeled as a random process without recourse to rocket dynamics in the former.

It should be kept in mind that these GT models cannot be expected to have good accuracy when the angle of attack is not small, not to mention the possibility of staging. Significant lateral forces (lateral to the velocity vector) do exist and sometimes cannot be neglected. In view of their strong temporal correlation, it seems reasonable in our opinion to incorporate into the total acceleration a stochastic model — such as the Singer (first-order Markov) model, similar to those for the lift — for the thrust (or more precisely, non-gravitational net) acceleration components that are normal to the velocity vector [45].

5.4 Example of A Profile-Based Model

All models discussed so far are profile-free. They describe the target motion by a state vector of a small dimension without recourse to additional information of the target trajectory. Most of these models (as seen above) are nonlinear and in general require numerical integration to propagate the trajectory. This is an intensive and hard computational task to implement in real time, especially when many targets are to be tracked simultaneously. Also, they do not guarantee satisfactory accuracy. As an alternative, a profile-dependent approach has been used traditionally in the BT tracking, where *trajectory profiles* are obtained *a priori* (off-line) to propagate the motion parameters in time [39, 49]. A trajectory profile (or template) typically consists of tabulated trajectory parameters [e.g., altitude, down-range and cross-range (in the orbital plane) position coordinates] as functions of time since launch. If an accurate profile is used, highly accurate estimates of the current target states can be obtained. In practice the exact profile of a foreign target of interest is not known (and may not even be in the set of available profiles) and is subject to ID determination (target typing). Usually it is searched among a set of profiles, calculated in advance for the target types of interest over a plausible range of their trajectory parameters. This process, generally referred to as profile (or template) matching, has a number of inherent issues to which specific techniques have been applied, which are beyond the scope of this survey.

Although much work has been done on profile-dependent modeling, relevant information available in the open literature is limited since target profile information is usually classified. We illustrate the idea via a simplified 2D model [50] used in such a framework. More detailed considerations of the approach can be found in [39, 49, 50, 9] and the references therein.

The target trajectory is assumed (common in the profile-based modeling) to remain approximately in a single (orbital) plane, defined by the position vector $\mathbf{p} = [x,\ y,\ z]'$ and velocity vector $\mathbf{v} = \dot{\mathbf{p}}$ in the ECI-CS. The pair of vectors $\left(\frac{\mathbf{p}}{\|\mathbf{p}\|},\ \frac{\mathbf{h}}{\|\mathbf{h}\|}\right)$ with $\mathbf{h} \triangleq \mathbf{v} - (\mathbf{v} \cdot \mathbf{p})\frac{\mathbf{p}}{\|\mathbf{p}\|}$ provides an orthonormal basis of this plane and determines the vertical and horizontal directions respectively. The net acceleration vector is then easily specified in the orbital plain as $\mathbf{a}_N = \alpha\left[\cos\varphi\frac{\mathbf{p}}{\|\mathbf{p}\|} + \sin\varphi\frac{\mathbf{h}}{\|\mathbf{h}\|}\right]$ through its magnitude α and orientation — the pitch-over angle $\varphi \triangleq \angle(\mathbf{a}_N, \mathbf{p})$ from the vertical. After accounting for the gravity, such as given in (48), the motion model in the ECI-CS is given by

$$\ddot{\mathbf{p}} = \left[\alpha(t)\cos\varphi(t) - \frac{\mu}{\|\mathbf{p}\|^2}\right]\frac{\mathbf{p}}{\|\mathbf{p}\|} + \alpha(t)\sin\varphi(t)\,\frac{\mathbf{h}}{\|\mathbf{h}\|} \tag{69}$$

where $\alpha(t)$ and $\varphi(t)$ are *known* functions of time. In such a case (given α and φ) the target state vector consists of only position and velocity components: $\mathbf{x} = [\mathbf{p}',\ \mathbf{v}']'$ and (69) yields a second-order nonlinear state-space model, which can be used to propagate the target state, e.g., by numerical integration.

The knowledge of $\alpha(t)$ and $\varphi(t)$ is a key assumption of this model, characteristic of the profile-based modeling. Thus a thrust profile is defined in [50] as a pair of curves $\mathcal{P} = \{(\alpha(t),\ \varphi(t)) : t_0 \le t \le t_f\}$, where t_0 and t_f denote the times of launch and final stage burnout respectively. A piecewise exponential model for $\alpha(t)$ and a linear model for $\varphi(t)$ were used in [50] to approximate the actual profiles.

As mentioned above this model is a simplified one. In a real-world application, other essential factors, such as the Earth-rotational effects (see Sec. 5.6.1 of [9] and [4]) and possible "out-of-plane" motions, should be accounted for.

Additional references concerning the profile-based booster modeling are [51, 52].

6 Modeling of BT Motion for Entire Trajectory

Evidently, different models have been developed for different regimes of a BT flight. In other words, no single model is adequate for most BT tracking applications, although it was reported in [5] that the first-order Markov (Singer) booster models of Sec. 5.2.2 performed reasonably well over the entire BT trajectories considered. Consequently, there is a need to decide on the proper model(s) to use at any given time when tracking a BT.

A natural idea is to use a decision logic — relying on e.g., target altitude, and possibly others — to determine the flight phase in effect at the time and use the corresponding (single) model for tracking. Albeit simple, it hinges on choosing the correct model, which is hard, particularly during a phase transition.

Alternatively and preferably, *multiple models* (MM) can be used simultaneously [38]. This approach was indeed taken and reported in [16, 42, 40, 9, 5]. Three classes of MM architectures, corresponding to the three generations of MM algorithms [53], have been proposed or used for BT tracking: *autonomous* MM (AMM) [16, 5], *interacting* MM (IMM) [42, 40, 9], and *variable-structure* MM (VSMM) [16, 5]. They all use a bank of elemental filters, each based on a particular model in the model set.

The multiple elemental filters in the AMM architecture are completely independent during the tracking process. The state estimate at any time is obtained from the one based on the most probable model at the time [16, 5], even though the state estimate of a *standard* AMM algorithm should be a probabilistically weighted sum of estimates from all elemental filters. As such, the model selection is done automatically according to the computed model probabilities and the estimated state trajectory is pieced together from segments of the estimated trajectories by the independent elemental filters.

In the IMM architecture [54, 38], the probabilistically weighted sums of estimates from all elemental filters are always taken to be the (overall) state estimates. More importantly, elemental filters interact one another by utilizing the most recent past estimates from every elemental filter. As such, the state estimates are in fact always a mixture of estimates based on all models, although with different weights.

A variable-structure MM uses a time-varying set of models. Although not formally stated in [16, 5], its MM-based tracking system actually uses a variable set of models (e.g., some models are deleted in real time), determined mostly by target altitude, and thus has a variable structure.

Another advantage of an MM-based tracker is that, as reported in [5], it allows the inclusion of certain "generic" (i.e., not phase specific) models for the end-to-end BT motion to provide a "back-up" in case other models in the working set do not work well, although these generic models may have degraded accuracy compared to the more definite phase-specific models.

It seems that a variable-structure IMM architecture is particularly suitable for BT tracking. A more detailed description of these MM algorithms, including their pros and cons is beyond the scope of this survey. The reader is referred to the recent surveys [55, 56, 53].

It should be emphasized that even when multiple models are used, inclusion of at least one accurate dynamics model for the flight phase in effect is still of vital importance for precision tracking.

7 Concluding Remarks

Numerous dynamics models of ballistic targets for tracking purposes have been developed. In essence, these models amount to various combinations of models for three different classes of force — thrust, aerodynamic forces, and gravity — at a variety of accuracy levels. Coast models consider gravity only; reentry models account for aerodynamical effects as well as gravity; and booster models rely on models for all three forces.

There are essentially three different gravity models used for BT tracking: the simplest constant-gravity model that assumes a flat, nonrotating Earth; the inverse-square model based on a spherical Earth; and the sophisticated model with the J_2 correction for an ellipsoidal Earth. These models are more universally applicable than models for other forces. The issue here is not a lack of sufficiently accurate models[19], but a choice of an appropriate model for the problem at hand. This choice depends mainly upon the intended coverage of the motion regime(s) and the affordable sophistication level. As a result, coast models require the most sophisticated, while relatively simpler ones can be used for boosters and reentry vehicles.

Aerodynamic forces include mainly drag and lift. The lift is responsible for maneuvers and, along its induced drag, is basically not predicable in the case of a foreign BT beyond the fact that the lift has to be in the plane normal to the velocity vector. Therefore, stochastic modeling techniques play an important role here. The state of the art here is at the level of the Singer model for aircraft maneuvers. In our opinion, many other stochastic models, particularly those of an adaptive nature, described in Sec. 4 of [1] have potentials here and deserve investigation. The zero-lift drag is relatively more predicable and its models rely heavily on aerodynamics. An improvement here calls for the adoption of a better yet affordable atmospheric model for pressure, temperature, air density, and so on.

The thrust is propellant specific and an accurate model that is generic enough is hard to come by. Available booster models either treat it entirely as a random process with a stochastic model or (but not both) impose simplifying constraints on it based on rocket dynamics. As stated at the end of Sec. 5.3, we believe a better model is to impose simplifying constraints and model the deviation from the constraints as a random process. In view of the similarity between the widely used gravity turn models for the boosters and the coordinated-turn models for aircraft maneuvers, attention should be paid to the advances in the latter, particularly in terms of kinematic constraints, for their applicability to the former.

The Coriolis and centrifugal forces arising from the rotation of the Earth exist only in a non-inertial frame. Its effects should be accounted for usually only when the BT under track is traveling over a large area or a long time period, such as the coast flight.

Compared with dynamics models of other powered-vehicles, BT models rely more on the aerodynamics and ballistics, and less on stochastic modeling techniques. While efforts for better modeling based on dynamics should continue, in our opinion, powerful stochastic modeling techniques deserve more attention in the future.

References

[1] X. R. Li and V. P. Jilkov. A Survey of Maneuvering Target Tracking: Dynamic Models. In *Proc. 2000 SPIE Conf. on Signal and Data Processing of Small Targets*, vol. 4048, pages 212–235, Orlando, Florida, USA, April 2000.

[2] X. R. Li and V. P. Jilkov. A Survey of Maneuvering Target Tracking—Part III: Measurement Models. In *Proc. 2001 SPIE Conf. on Signal and Data Processing of Small Targets*, vol. 4473, San Diego, CA, USA, 2001.

[3] A. Miele. *Flight Mechanics, Volume 1: Theory of Flight Paths*. Addison-Wesley, Reading, MA, 1962.

[4] R. R. Bate, D. D. Mueller, and J. E. White. *Fundamentals of Astrodynamics*. Dover Publications, 1971.

[5] P. F. Easthope. Using TOTS for More Accurate and Responsive Multi-Sensor, End-to-End Ballistic Missile Tracking. In *Proc. SPIE Conf. on Signal and Data Processing of Small Targets 2000*, vol. 4048, Apr. 2000.

[6] R. K. Mehra. A Comparison of Several Nonlinear Filters for Reentry Vehicle Tracking. *IEEE Trans. Automatic Control*, AC-16:307–319, Aug. 1971.

[19] Models more accurate than the above three are available, which have an accuracy beyond the need for tracking a ballistic target.

[7] F. E. Daum and R. J. Fitzgerald. Decoupled Kalman Filters for Phased Array Radar Tracking. *IEEE Trans. Automatic Control*, AC-28:269–282, Mar. 1983.

[8] S. S. Blackman. *Multiple Target Tracking with Radar Applications*. Artech House, Norwood, MA, 1986.

[9] S. S. Blackman and R. F. Popoli. *Design and Analysis of Modern Tracking Systems*. Artech House, Norwood, MA, 1999.

[10] J. R. Moore and W. D. Blair. Practical Aspects of Multisensor Tracking. In Y. Bar-Shalom and W. D. Blair, editors, *Multitarget-Multisensor Tracking: Applications and Advances*, vol. III, pages 1–76. Artech House, 2000.

[11] P. J. Costa. Adaptive Model Architecture and Extended Kalman-Bucy Filters. *IEEE Trans. Aerospace and Electronic Systems*, AES-30(2):525–533, April 1994.

[12] H. W. Sorenson. Kalman Filtering Techniques. In C. T. Leondes, editor, *Advances in Control Systems Theory and Applications*, volume 3, pages 219–292. Academic Press, New York, 1966. Also in [57], pp. 90-126.

[13] A. H. Jazwinski. *Stochastic Processes and Filtering Theory*. Academic Press, New York, 1970.

[14] T. H. Kerr. Streamlining Measurement Iteration for EKF Target Tracking. *IEEE Trans. Aerospace and Electronic Systems*, AES-27(2):408–421, March 1991.

[15] J. A. Roecker. Track Monitoring When Tracking With Multiple 2-D Passive Sensors. *IEEE Trans. Aerospace and Electronic Systems*, 27(6):872–875, 1991.

[16] P. F. Easthope and N. W. Heys. Multiple-Model Target-Oriented Tracking System. In *Proc. SPIE Conf. on Signal and Data Processing of Small Targets 2000*, vol. 2235, Apr. 1994.

[17] M. Yeddanapudi, Y. Bar-Shalom, Y. Pattipati, and S. Deb. Ballistic Missile Track Initiation from Satelite Observations. *IEEE Trans. Aerospace and Electronic Systems*, 31(3):1054–1071, July 1995.

[18] J. A. Lawton, R. J. Jesionowski, and P. Zarchan. Comparison of Four Filtering Options for a Radar Tracking Problem. *AIAA Journal of Guidance, Control and Dynamics*, 21(4):618–623, July-Aug. 1998.

[19] Y. Bar-Shalom and X. R. Li. *Multitarget-Multisensor Tracking: Principles and Techniques*. YBS Publishing, Storrs, CT, 1995.

[20] Y. Bar-Shalom and X. R. Li. *Estimation and Tracking: Principles, Techniques, and Software*. Artech House, Boston, MA, 1993. (Reprinted by YBS Publishing, 1998).

[21] R. K. Mehra. Approaches to Adaptive Filtering. *IEEE Trans. Automatic Control*, AC-17(5):693–698, Oct. 1972.

[22] X. R. Li and Y. Bar-Shalom. A Recursive Multiple Model Approach to Noise Identification. *IEEE Trans. Aerospace and Electronic Systems*, AES-30(3):671–684, July 1994.

[23] M. E . Hough. Improved Performance of Recursive Tracking Filters Using Batch Initialization and Process Noise Adaptation. *AIAA Journal of Guidance, Control, and Dynamics*, 22(5):675–681, 1999.

[24] G. P. Cardillo, A. V. Mrstik, and T. Plambeck. A Track Filter for Reentry Objects with Uncertain Drag. *IEEE Trans. Aerospace and Electronic Systems*, AES-35(2):395–409, Apr. 1999.

[25] C. B. Chang. Ballistic Trajectory Estimation with Angle Only Measurements. *IEEE Trans. Automatic Control*, AC-25:474–480, June 1980.

[26] F. J. Regan and S. M. Anandakrishnan. *Dynamics of Atmospheric Re-Entry*. AIAA, New York, 1993.

[27] N. Morrison. *Introduction to Sequential Smoothing and Prediction*. McGraw-Hill, New York, 1969.

[28] E. Brookner. *Tracking and Kalman Filtering Made Easy*. John Wiley & Sons, Inc.,, New York, 1989.

[29] G. M. Siouris, G. Chen, and J. Wang. Tracking an Incoming Ballistic Missile Using an Extended Interval Kalman Filter. *IEEE Trans. Aerospace and Electronic Systems*, AES-33(1):232–240, Jan. 1997.

[30] P. Zarchan. *Tactical and Strategic Missile Guidance*. AIAA, Washington DC, Aug. 1998.

[31] C. B. Chang, R. H. Whiting, and M. Athans. On the State and Parameter Estimation for Maneuvering Reentry Vehicles. *IEEE Trans. Automatic Control*, AC-22(2):99–105, Feb. 1977.

[32] R. P. Wishner, R. E. Larson, and M. Athans. Status of Radar Tracking Algorithms. In *Proc. Symp. Nonlinear Estimation*, San Diego, CA, Sept. 1970.

[33] R. J. Fitzgerald. On Reentry Vehicle Tracking in Various Coordinate Systems. *IEEE Trans. Automatic Control*, AC-19:581–582, July 1974.

[34] M. E. Hough. Optimal Guidance and Nonlinear Estimation for Interception of Decelerating Targets. *AIAA Journal of Guidance, Control, and Dynamics*, 18(2):316–324, 1995.

[35] C. B. Chang and J. Tabaczynski. Application of State Estimation to Target Tracking. *IEEE Trans. Automatic Control*, AC-29(2):98–109, Feb. 1984.

[36] S.-C. Lee and C.-Y. Liu. Trajectory Estimation of Reentry Vehicle by Use of on-Line Input Estimator. *Journal of Guidance, Control, and Dynamics*, 22(6):808–815, 1999.

[37] Y. T. Chan, A. G. C. Hu, and J. B. Plant. A Kalman Filter Based Tracking Scheme with Input Estimation. *IEEE Trans. Aerospace and Electronic Systems*, AES-15(2):237–244, Mar. 1979.

[38] Y. Bar-Shalom, X. R. Li, and T. Kirubarajan. *Estimation with Applications to Tracking and Navigation: Theory, Algorithms, and Software*. Wiley, New York, 2001.

[39] J. G. Rudd, R. A. Marsh, and J. A. Roecker. Surveillance and Tracking of Ballistic Missile Launches. *IBM Journal of Research and Development*, 38(2):195–216, March 1994.

[40] M. Miller, O. Drummond, and A. Perrella. Multiple-Model Filters for Boost-to-Coast Transtition of Theater Ballistic Missiles. In *Proc. 1998 SPIE Conf. on Signal and Data Processing of Small Targets*, vol. 3373, pages 355–376, 1998.

[41] K.-H. Keil. Generic Case Study: Evaluation of Early Warning Satellites Cueing Radars against TBM. In *Proc. 1999 SPIE Conf. on Signal and Data Processing of Small Targets*, vol. 3809, pages 297–37, Denver, CO, USA, July 1999.

[42] E. Svestins. Multi-Radar Tracking for Theater Missile Defence. In *Proc. 1995 SPIE Conf. on Signal and Data Processing of Small Targets*, vol. 2561, pages 384–394, San Diego, CA, July 1995.

[43] R. G. Hutchins and A. San Jose. IMM Tracking of a Theater Ballistic Missile during Boost Phase. In *Proc. 1998 SPIE Conf. on Signal and Data Processing of Small Targets*, vol. 3373, pages 528–531, Orlando, FL, Apr. 1998.

[44] R. G. Hutchins and A. San Jose. Trajectory Tracking and Backfitting Techniques Against Theater Ballistic Missiles. In *Proc. 1999 SPIE Conf. on Signal and Data Processing of Small Targets*, vol. 3809, pages 532–526, Denver, CO, July 1999.

[45] V. P. Jilkov, X. R. Li, and J.-F. Ru. Modeling of Gravity-Turn Motion for Ballistic Target Tracking. To be submitted for publication, 2001.

[46] M. E. Hough. Optimal Guidance and Nonlinear Estimation for Interception of Accelerating Targets. *AIAA Journal of Guidance, Control, and Dynamics*, 18(5):958–968, 1995.

[47] J. L. Fowler. Boost and Post-Boost Target State Estimation with Angles-Only Measurements in a Dynamic Spherical Coordinate System. In *Proc. of AAS/AIAA Astrodynamics Conf.*, pages 41–54, Aug. 19-21 1991.

[48] W. A. Fisher and H.E. Rauch. Augmentation of an Extended Kalman Filter with a Neural Network. In *Proc. 1994 IEEE Int. Conf. on Neural Networks*, pages 1191–1196, Orlando, FL, June 1994.

[49] N.J. Danis. Space-Based Tactical Ballistic Missile Launch Parameter Estimation. *IEEE Trans. Aerospace and Electronic Systems*, AES-29(2):412–424, April 1993.

[50] M. Yeddanapudi and Y. Bar-Shalom. Trajectory Prediction for Missiles Based on Boost-Phase LOS Measurements. In *Proc. 1997 SPIE Conf. on Signal and Data Processing of Small Targets*, vol. 3163, pages 316–328, July 1997.

[51] M. Tsai and F.A. Rogel. Angle-Only Tracking and Prediction of Boost Vehicle Position. In *Proc. SPIE on Signal and Data Processing for Small Targets*, vol. 1481, 1991.

[52] E. Woods and T. Queeney. Multisensor Detection and Tracking of Tactical Ballistic Missiles Using Knowledge-Based State Estimation. In *Proc. SPIE Signal Processing, Sensor Fusion and Target Recognition III*, vol. 2232, 1994.

[53] X. R. Li. Engineer's Guide to Variable-Structure Multiple-Model Estimation for Tracking. In Y. Bar-Shalom and D. W. Blair, editors, *Multitarget-Multisensor Tracking: Applications and Advances*, volume III, chapter 10, pages 499–567. Artech House, Boston, MA, 2000.

[54] H. A. P. Blom and Y. Bar-Shalom. The Interacting Multiple Model Algorithm for Systems with Markovian Switching Coefficients. *IEEE Trans. Automatic Control*, AC-33(8):780–783, Aug. 1988.

[55] X. R. Li. Hybrid Estimation Techniques. In C. T. Leondes, editor, *Control and Dynamic Systems: Advances in Theory and Applications*, volume 76, pages 213–287. Academic Press, New York, 1996.

[56] E. Mazor, A. Averbuch, Y. Bar-Shalom, and J. Dayan. Interacting Multiple Model Methods in Target Tracking: A Survey. *IEEE Trans. Aerospace and Electronic Systems*, AES-34(1):103–123, 1996.

[57] H. W. Sorenson, editor. *Kalman Filtering: Theory and Application*. IEEE Press, 1985.